THE JOURNAL OF BIOLOGICAL CHEMISTRY VOL. 289, NO. 41, pp. 28338–28351, October 10, 2014

Roles for N-terminal Extracellular Domains of Nicotinic Acetylcholine Receptor (nAChR) β3 Subunits in Enhanced Functional Expression of Mouse α6β2β3- and α6β4β3-nAChRs*

Received for publication, March 15, 2014, and in revised form, June 27, 2014 Published, JBC Papers in Press, July 15, 2014, DOI 10.1074/jbc.M114.566018

Bhagirathi Dash[‡], **Ming D. Li**[‡], **and Ronald J. Lukas**[§1]

From the [‡]*Department of Psychiatry and Neurobehavioral Sciences, School of Medicine, University of Virginia, Charlottesville, Virginia 22911 and* [§]*Division of Neurobiology, Barrow Neurological Institute, Phoenix, Arizona 85013*

Background: Naturally expressed mouse (m) α6*-nAChRs have negligible functional expression *in vitro*.
Results: Functional expression of mouse α6β2β3- or α6β4β3-nAChRs is enhanced upon manipulation of β3 subunit N-terminal extracellular domain residues.
Conclusion: N-terminal extracellular domains in nAChR β3 subunits play heretofore underappreciated roles in controlling functional expression of α6*-nAChR.
Significance: nAChR "accessory" subunits are critical elements in nAChR assembly and function.

Functional heterologous expression of naturally expressed mouse α6*-nicotinic acetylcholine receptors (mα6*-nAChRs; where "*" indicates the presence of additional subunits) has been difficult. Here we expressed and characterized wild-type (WT), gain-of-function, chimeric, or gain-of-function chimeric nAChR subunits, sometimes as hybrid nAChRs containing both human (h) and mouse (m) subunits, in *Xenopus* oocytes. Hybrid mα6mβ4hβ3- (~5–8-fold) or WT mα6mβ4mβ3-nAChRs (~2-fold) yielded higher function than mα6mβ4-nAChRs. Function was not detected when mα6 and mβ2 subunits were expressed together or in the additional presence of hβ3 or mβ3 subunits. However, function emerged upon expression of mα6mβ2mβ3$^{V9'S}$-nAChRs containing β3 subunits having gain-of-function V9′S (valine to serine at the 9′-position) mutations in transmembrane domain II and was further elevated 9-fold when hβ3$^{V9'S}$ subunits were substituted for mβ3$^{V9'S}$ subunits. Studies involving WT or gain-of-function chimeric mouse/human β3 subunits narrowed the search for domains that influence functional expression of mα6*-nAChRs. Using hβ3 subunits as templates for site-directed mutagenesis studies, substitution with mβ3 subunit residues in extracellular N-terminal domain loops "C" (Glu^{221} and Phe^{223}), "E" (Ser^{144} and Ser^{148}), and "β2-β3" (Gln^{94} and Glu^{101}) increased function of mα6mβ2*- (~2–3-fold) or mα6mβ4* (~2–4-fold)-nAChRs. EC$_{50}$ values for nicotine acting at mα6mβ4*-nAChR were unaffected by β3 subunit residue substitutions in loop C or E. Thus, amino acid residues located in primary (loop C) or complementary (loops β2-β3 and E) interfaces of β3 subunits are some of the molecular impediments for functional expression of mα6mβ2β3- or mα6mβ4β3-nAChRs.

Nicotinic acetylcholine receptors (nAChRs)[2] are a diverse set of pentameric, transmembrane, signal-transducing proteins found in the nervous system and elsewhere. Vertebrate nAChR subunits α1–α10, β1–β4, γ, δ, and ϵ are encoded from a family of distinct genes. α1, β1, δ, and either γ or ϵ subunits form muscle-type nAChRs, and other nAChR subtypes are formed as heteromers or homomers of the remaining subunits (1). Homomeric α7-nAChRs and heteromeric α4β2- or α6β2*-nAChRs (* indicates the known or possible presence of additional subunits) are the dominant subtypes in the central nervous system (CNS) (2). α6β4*-nAChRs do not seem to be abundant in the rodent CNS but are found in rat dorsal root ganglion neurons and in human adrenal chromaffin cells (3, 4). α6*-nAChRs seem to participate in the modulation of dopamine release, locomotion, reward, and reinforcement and have been implicated in schizophrenia and Parkinson disease (5–12).

Beyond the known formation of α6β2- or α6β4-nAChRs (3, 4, 13–15), integration of nAChR α4, β3, or α5 subunits can occur (14–17) to yield more complex α6*-nAChR subtypes. nAChR β3 or α5 subunits have been classified as "accessory" subunits because they do not form functional receptors alone or seem to combine with any other single kind of nAChR α or β subunit in a functional way, but they can participate in trinary complexes containing other, selected α and β subunits (15, 18–22). Integration of nAChR β3 subunits in the accessory

* This work was supported, in whole or in part, by National Institutes of Health Grant R01 DA012844 and DA026356 (to M. D. L.) and DA015389 (to R. J. L.). This work was also supported by endowment and capitalization funds from the Barrow Neurological Foundation (to R. J. L.) and the External Research Program of Philip Morris USA Inc. and Philip Morris International (to R. J. L.). Portions of this work have been presented in abstract form: Dash, B., Bhakta, M., Whiteaker, P., Stitzel, J. A., Chang, Y., and Lukas, R. J. (2009) Gain-of-function mutants in human or mouse nAChR β3 subunits interchangeably activate either human or mouse α6β4*-nAChR but not human or mouse α6β2*-nAChR. *Soc. Neurosci. Abstr.* **35,** 34.7.
[1] To whom correspondence should be addressed: Division of Neurobiology, Barrow Neurological Inst., 350 W. Thomas Rd., Phoenix, AZ 85013. Tel.: 602-406-3399; Fax: 602-406-4172; E-mail: Ronald.Lukas@DignityHealth.org.

[2] The abbreviations used are: nAChR, nicotinic acetylcholine receptor; ACh, acetylcholine; I_{max}, peak current response; h, human; m, mouse; AA, amino acid; TM, transmembrane domain; NTD, N-terminal domain; RC, reverse complement.

TABLE 1

Primers and restriction sites used to create mutant/chimeric constructs

For mutants, the first amino acid (single letter code; numbering begins at the translation start methionine) designates the wild-type nAChR (human or mouse) subunit residue that is replaced with the indicated second amino acid. In the forward primer nucleic acid sequence, capitalization indicates the nucleotide(s) changed from the wild-type subunit to create the corresponding mutant or restriction site.

Primer	Mutant	Forward primer sequences
P1	hβ3_V181_SalI	5′-cttatgatggcaccatggtCgacctcattttgatcaatg-3′
	mβ3_Val187_SalI	Innate
	mβ3_BglII	Innate
	hβ3_BglII	Innate
P2	mβ3_R375_BsiWI	5′-gagagtaagggaaccgtACgggggaaatttccaggg-3′
P3	hβ3_K369_BsiWI	5′-ccagagaaagaggagagtcaaccagtCgtACGaggcaaagtcctcgaaaaaaagaaac-3′
P4	mβ3 (V279S)[a]	5′-cacctcggttttgTCttctttgacagtg-3′
P5	hβ3 (V273S)[a]	5′-cattatccacatcggtcttgTCttctctgacagttttcc-3′
P6	mβ3 (Q94H)	5′-caggaatggacagaccaTaaattacgatggaatccc-3′
P7	mβ3 (E101D)	5′-caaaaattacgatggaatcccgaTgactatggtggaattaattcg-3′
P8	mβ3 (N107H)	5′-ccgaagactatggtggaattCattcgataaaggttccatc-3′
P9	mβ3 (Q94H/E101D)	5′-caTaaattacgatggaatcccgaTgactatggtggaattaattcg-3′
	mβ3 (Q94H/N107H)	Use P8 on nAChR mβ3 (Q94H) construct
P10	mβ3 (S144N/S148V)	5′-ctcatgaccaaggccattgtgaaatccaAcggaaccgtcGgttggactcctcccgccagctacaaaag-3′
P11	mβ3 (E221D)	5′-gaagggcaacagaagagaCggcttttactcctatccg-3′
P12	mβ3 (E221D/F223V)	5′-gggatgaagggcaacagaagagaCggcGtttactcctatccgtttgttacc-3′

[a] Primer created and used before (15).

position is suggested to be a critical, final step in formation, assembly, and stability of mature α6β3*-nAChRs (6, 23) and is important for function of α6*- and other nAChRs (24–31). A positive role of the β3 subunit, rather than a negative role (27), in the function of α6*-nAChRs has been revealed from knockout animal studies (6). However, structure-function relationships and pharmacological features of α6*-nAChRs are poorly understood because receptors thought to exist naturally have not been easily recreated in heterologous expression systems (13–15, 20).

There have been some successes in expressing functional α6*-nAChRs using *Xenopus* oocytes (22) or cell lines when a chimeric nAChR (α6/α3) subunit (composed of the α6 subunit extracellular N-terminal domain fused to an otherwise α3 subunit) was used instead of the wild-type (WT) nAChR α6 subunit (32) or when enhanced GFP-tagged α6- and β2-nAChR subunits were coexpressed in Neuro-2a cells (13). Other strategies have been to use gain-of-function variants of β3 or α5 subunits (typically using subunits mutated to express serine instead of valine at the so-called 9′-position in the subunit channel-lining, second transmembrane domain (TM II); V9′S) to express functional α6*-nAChRs in *Xenopus* oocytes (15, 27). We also recently succeeded in producing functional, hybrid α6β3*-nAChRs substituting mouse (m) α6 subunits for human (h) α6 subunits to express functional mα6hβ4hβ3- or mα6hβ2hβ3$^{V9'S}$-nAChRs (15). This kind of study leveraging innate variations in amino acid (AA) residues between subunits from different species produced valuable information regarding structure and function of invertebrate and vertebrate nAChRs (15, 21, 33, 34).

Here we report that nAChR hβ3 or hβ3$^{V9'S}$ (*i.e.* hβ3(V273S)) subunits coexpressed in oocytes also expressing mα6 subunits in the presence of mβ4 or mβ2 subunits yielded nAChRs with higher levels of function than those of mα6mβ4mβ3- or mα6mβ2mβ3$^{V9'S}$-nAChRs. Further studies using chimeric or gain-of-function chimeric mouse/human nAChR β3 subunits and site-directed mutagenesis identified AA residues in the extracellular N-terminal domain (NTD; in so-called loops "β2-β3," C, and E) of mβ3 subunits that when substituted with corresponding residues from hβ3 subunits alone or in some specific combinations increased the function of mα6mβ2*- and mα6mβ4*-nAChRs. These studies elucidate some of the structural bases dictating roles for nAChR β3 subunits in functional expression of mα6mβ2*- and mα6mβ4*-nAChRs.

EXPERIMENTAL PROCEDURES

Bioinformatics and Homology Modeling—Using several Web-available threading methods, the β1 subunit of the muscle nicotinic acetylcholine receptor of the marbled electric ray (*Torpedo marmorata*) (2BG9.B; Protein Data Bank code 2BG9 Chain B) (35) was identified as a suitable template for three-dimensional modeling of mβ3 subunits (SWISS-MODEL Protein Modeling Server) (36). The overall stereochemical quality of the final model was assessed by the program PROCHECK (37). The homology model for the nAChR mβ3 subunit was rendered using UCSF Chimera, a program for interactive visualization and analysis of molecular structures. Protein sequences for nAChR β3 subunits of several species or mouse nAChR subunits retrieved from the National Center for Biotechnology Information (NCBI) Entrez Web service were aligned with each other using the Web program ClustalW.

Chemicals—All chemicals for electrophysiology were obtained from Sigma. Fresh agonist (acetylcholine (ACh) or nicotine) or antagonist (atropine) stock solutions were made daily or diluted from frozen stock in Ringer's solution (OR2), which consisted of 92.5 mM NaCl, 2.5 mM KCl, 1 mM $CaCl_2$, 1 mM $MgCl_2$, and 5 mM HEPES, pH 7.5.

Wild-type nAChR Subunits—nAChR hβ3, mα6, mβ2, mβ3, and mβ4 subunits were subcloned into the oocyte expression vector pGEMHE as described previously (19, 30).

nAChR β3 Subunit Chimeras—Guided by an alignment of nAChR hβ3 and mβ3 subunit protein sequences (see Fig. 1*A*), chimeric mouse/human β3 subunits were designed and created (see Fig. 1*B*) as described below. We cared to construct chimeras in a manner that isolated domains and/or structural features in β3 subunits.

Construction of the mβ3(1–187)/hβ3(182–458) Chimeric Subunit (SalI Site-based Construct)—Mouse nAChR β3 subunits possess an innate SalI restriction site (see Fig. 1) in the NTD around AA residue Val[187]. A SalI restriction site (Table 1)

was created in the pGEMHE-hβ3 construct (*i.e.* pGEMHE-hβ3(SalI)) by site-directed mutagenesis around AA residue Val^{181} by using primers P1 (forward) and its reverse complement (RC) (Table 1). Both pGEMHE-mβ3 and pGEMHE-hβ3(SalI) constructs were digested with SalI and XbaI where the XbaI site is located downstream of the sequence encoding the C-terminal end of the mβ3 or hβ3 cDNA and is in the multiple cloning site. The pGEMHE-mβ3(XbaI+SalI) (*i.e.* mβ3(1–187)) and hβ3(SalI+XbaI) (*i.e.* hβ3(182–458)) cDNA fragments were gel-purified and ligated, producing a chimeric cDNA construct pGEMHE-mβ3(1–187)/hβ3(182–458) (*i.e.* mβ3(Met^1–Val^{187})/hβ3(Asp^{182}–His^{458})) (see Fig. 1).

Construction of the mβ3(1–329)/hβ3(324–458) Chimera (BglII Site-based Construct)—Both human and mouse β3 subunits possess an innate BglII restriction site right after the third transmembrane domain (TM III). The BglII site allows cutting through human and mouse β3 cDNA at equivalent and homologous residues (see Fig. 1). Both pGEMHE-mβ3 and pGEMHE-hβ3 plasmids were double digested with BglII and XbaI. pGEMHE-mβ3(XbaI+BglII) (*i.e.* mβ3(1–329)) and hβ3(BglII-XbaI) (*i.e.* hβ3(324–458)) cDNA fragments were gel-purified and ligated to produce the chimeric construct pGEMHE-mβ3(1–329)/mβ3(324–458) (*i.e.* mβ3(Met^1–Arg^{329})/hβ3(Ser^{324}–His^{458})) (see Fig. 1). This chimera could be considered as a combination of the NTD of mβ3 subunit and the rest of the hβ3 subunit because the AA residues between the 239th residue (presumably its N-terminal end) and the BglII site in the mβ3 subunit are identical to those between the 233rd residue (presumably its N-terminal end) and the BglII site in the hβ3 subunit (see Fig. 1).

Construction of the mβ3(1–375)/hβ3(370–458) Chimera (BsiWI Site-based Construct)—A BsiWI restriction site around AA residue Arg^{375} in pGEMHE-mβ3 (using P2 and its RC; Table 1) and another one around AA residue Lys^{369} in pGEMHE-hβ3 (using P3 and its RC) were created by site-directed mutagenesis (Table 1). Both pGEMHE-mβ3(BsiWI) and pGEMHE-hβ3(BsiWI) plasmids were double digested with BsiWI and XbaI. pGEMHE-mβ3(XbaI+BsiWI) (*i.e.* mβ3(1–375)) and hβ3(BsiWI+XbaI) (*i.e.* hβ3(370–458)) cDNA fragments were gel-purified and ligated to produce the chimeric pGEMHE-mβ3(1–375)/hβ3(370–458) (*i.e.* mβ3(Met^1–Arg^{375})/hβ3(Gly^{370}–His^{458})) (see Fig. 1).

Gain-of-function Chimeric nAChR β3 Subunits—TM II 9′ valine-to-serine (V9′S) mutations in pGEMHE-mβ3(1–329)/hβ3(324–458) and pGEMHE-mβ3(1–375)/hβ3(370–458) constructs were introduced using primer P4 (Table 1) and its RC to produce pGEMHE-mβ3(1–329)^{V279S}/hβ3(324–458) and pGEMHE-mβ3(1–375)^{V279S}/hβ3(370–458) constructs, respectively (Fig. 1). Similarly, TM II V9′S mutations in the pGEMHE-mβ3(1–187)/hβ3(182–458) construct were introduced using primer P5 (Table 1) and its RC to produce the pGEMHE-mβ3(1–187)/hβ3(182–458)^{V273S} construct.

Point Mutants—TM II V9′S, L9′S, or V13′S mutations in hβ3 (V9′S = V273S; V13′S = V277S), mβ3 (V9′S = V279S; V13′S = V283S), or mα6 (L9′S = L280S; V13′S = V284S) subunits were introduced into the pGEMHE background using the QuikChange II site-directed mutagenesis kit (Stratagene, La Jolla, CA) as described previously (15, 38).

Single or double mutations in nAChR mβ3 subunit (*i.e.* Q94H, E101D, N107H, Q94H/E101D, S144N/S158V, E221D, and E221D/F223V) were introduced using the QuikChange II site-directed mutagenesis kit using their respective forward (P6, P7, P8, P9, P10, P11, and P12; Table 1) and RC primers. The pGEMHE-mβ3(Q94H/N107H) construct was made by site-directed mutagenesis of the pGEMHE-mβ3(Q94H) construct using primer P8 and its RC.

TM II 9′ valine-to-serine mutations in plasmids encoding mβ3(Q94H), mβ3(E101D), mβ3(N107H), mβ3(Q94H/E101D), mβ3(Q94H/N107H), mβ3(S144N/S158V), mβ3(E221D), or mβ3(E221D/F223V) subunits were introduced using primer P4 (Table 1) and its RC. Construct integrity and accuracy of all subunits were confirmed by DNA sequencing.

Complementary RNA (cRNA) Preparation—All pGEMHE plasmids were linearized immediately downstream of the 3′-polyadenylation sequence. NheI was used to linearize hβ3, hβ3$^{V9'S}$, hβ3$^{V13'S}$, mα6, mα6$^{L9'S}$, mα6$^{V13'S}$, mβ2, mβ3$^{V9'S}$, mβ4, mβ3(1–187)/hβ3(182–458), mβ3(1–329)/hβ3(324–458), mβ3(1–375)/hβ3(370–458), mβ3(1–187)/hβ3(182–458)^{V273S}, mβ3(1–329)^{V279S}/hβ3(324–458), mβ3(1–375)^{V279S}/hβ3(370-458), mβ3(Q94H), mβ3(E101D), mβ3(N107H), mβ3(Q94H/E101D), mβ3(Q94H/N107H), mβ3(S144N/S158V), mβ3(E221D), mβ3(E221D/F223V), mβ3(Q94H)$^{V9'S}$, mβ3(E101D)$^{V9'S}$, mβ3-(N107H)$^{V9'S}$, mβ3(Q94H/E101D)$^{V9'S}$, mβ3(Q94H/N107H)$^{V9'S}$, mβ3(S144N/S158V)$^{V9'S}$, mβ3(E221D)$^{V9'S}$, and mβ3(E221D/F223V)$^{V9'S}$ subunit-encoding plasmids. Capped, full-length cRNAs were prepared using individual reaction components as detailed earlier (19) or using the mMESSAGE mMACHINE® T7 kit (Ambion Inc./Invitrogen) following the manufacturer's instructions. The integrity and quality of the cRNAs were checked by electrophoresis and UV spectroscopy prior to cRNA injection.

Preparation of cRNA Mixtures for Injection—We planned to introduce identical amounts of cRNA, presumably producing equal amounts of each subunit protein, into oocytes largely due to lack of information about the levels of mRNA for each subunit that composes α6*-nAChRs in neurons or cells. We provisionally assumed that α6 subunits or their mutants in association with β2 or β4 subunits would form complexes having 2:3 and/or 3:2 ratios of the indicated subunits and that oocytes also injected with WT, chimeric, or other forms of β3 subunits would express nAChR with 2:2:1 ratios of α:β:β3 subunits. For expression of binary nAChRs (*i.e.* nAChRs containing two subunits; α + β but not β3), cRNA mixtures were prepared by mixing 1 μl of cRNA for each subunit and an additional microliter of RNase-free water (*i.e.* total volume, 3 μl). Similarly, for expression of trinary nAChRs (*i.e.* nAChRs containing three subunits; (α + β) + β3) cRNA mixtures were prepared by mixing 1 μl of cRNA for each subunit. Several preparations of each cRNA mixture were prepared and stored at −80 °C until further use.

cRNA concentrations for each nAChR α and β subunit were adjusted to 150 ng/μl for the first set of experiments (for data presented in Table 2 and Fig. 2). As noted above, introduction of 69 nl of cRNAs (from a 3-μl cRNA mixture) into each oocyte would deliver ~3.5 ng of cRNA for each α and β subunit whether binary or trinary nAChRs are expressed. For all other

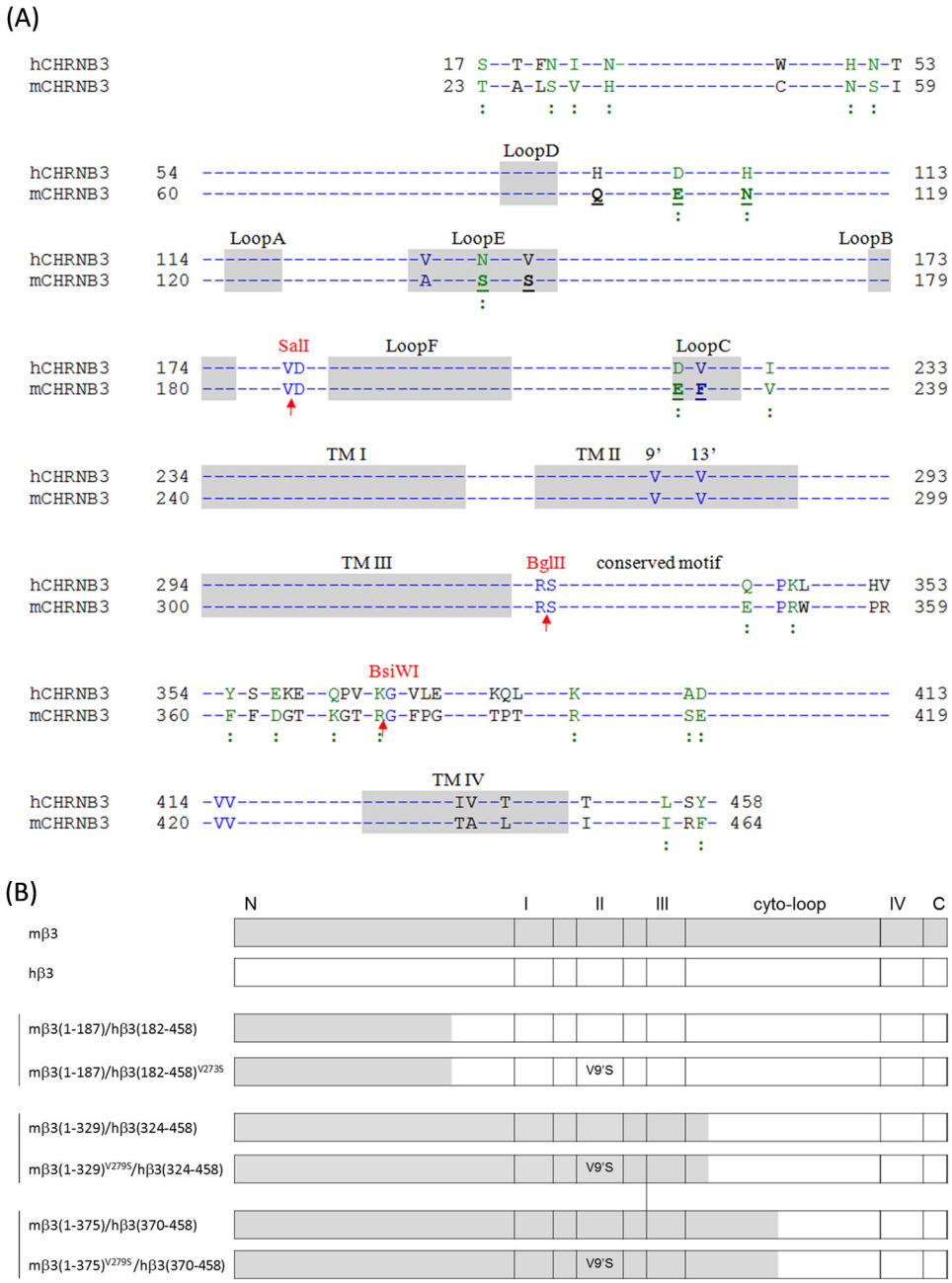

FIGURE 1. **Construction of nAChR β3 subunit chimeras.** *A*, alignment of nAChR hβ3 and mβ3 subunit protein sequences. Amino acid sequences of nAChR hβ3 (accession number NP_000740.1) and mβ3 subunits (accession number AAL75573.1) retrieved from GenBank™ were aligned using protein BLAST. AA numbering begins at the translation start methionine. Identical residues between human and mouse nAChR β3 subunits are indicated by a *dash* (-). Putative loop regions (A, B, and C in the primary face and D, E, and F in the complementary face), TM domains (I, II, III, and IV), and TM II 9′ and 13′ amino acid residues in human and mouse nAChR β3 subunits are identified. nAChR mβ3 subunit residues (Gln[94], Glu[101], Asn[107], Ser[144], Ser[148], Asp[221], and Phe[223]) given prime attention in mutagenesis studies are *underlined* and in *boldface*. An *upward arrow* (↑) indicates junctions for chimeric subunits and the restriction sites used for construction of chimeric mouse/human β3 subunits. *Colons* (:) below sequences indicate conserved residues. *B*, schematic diagrams of chimeric nAChR β3 subunits. Chimeric mouse/human nAChR β3 subunits with or without V9′S mutations in their respective TM II were constructed. The 273rd AA in nAChR hβ3 subunit or the 279th AA in nAChR mβ3 subunit is a valine and is noted as the 9′ AA in TM II. *N*, N-terminal domain; *I*, *II*, *III*, or *IV*, respective TM domains; *cyto-loop*, cytoplasmic loop; *C*, C terminus. *Numbers* in *brackets* are the regions of the indicated subunits that are used for construction of mouse/human β3 chimeric subunits.

experiments, concentrations of cRNAs prepared for each nAChR α and β subunit were adjusted to 500 ng μl^{-1}. Injection of 138 nl of cRNA of a 3-μl cRNA mixture into each oocyte would deliver ~23 ng of cRNAs for each α and β subunit whether binary or trinary nAChRs are expressed.

Oocyte Preparation and cRNA Injection—Female *Xenopus laevis* (*Xenopus* I, Ann Arbor, MI or Nasco, Fort Atkinson, WI) were anesthetized using 0.2% tricaine methanesulfonate (MS-222) (Sigma or Nasco). Ovarian lobes were surgically removed from the frogs and placed in an incubation solution that consisted of 82.5 mM NaCl, 2.5 mM KCl, 1 mM $MgCl_2$, 1 mM $CaCl_2$, 1 mM Na_2HPO_4, 0.6 mM theophylline, 2.5 mM sodium pyruvate, 5 mM HEPES, 50 mg/ml gentamycin, 50 units/ml penicillin, and 50 μg/ml streptomycin, pH 7.5. The lobes were cut into small pieces and digested with 0.08 Wünsch units/ml Liberase Blendzyme 3 (Roche Applied Science) with constant stirring at room

temperature for 1.5–2 h. The dispersed oocytes were thoroughly rinsed with incubation solution. Stage VI oocytes were selected and incubated at 16 °C before injection. Micropipettes used for injection were pulled from borosilicate glass (Drummond Scientific, Broomall, PA) using a Sutter P87 or P1000 horizontal puller (Sutter Instrument Co., Novato, CA), and the tips were broken with forceps to ~40 μm in diameter. cRNAs were drawn up into the micropipette and injected into oocytes using a Nanoject or Nanoject II microinjection system (Drummond Scientific) at a total volume of 69 or 138 nl.

Oocyte Electrophysiology—Two to 5 days after injection, oocytes were placed in a small volume chamber and continuously perfused with OR2. The chamber was grounded through an agarose bridge. The oocytes were voltage-clamped at −70 mV (unless otherwise noted) to measure agonist- or antagonist-induced currents using Axoclamp 900A and pClamp 10.2 software (Axon Instruments/Molecular Devices, Sunnyvale, CA). The current signal was low pass-filtered at 10 Hz with the built-in low pass Bessel filter in the Axoclamp 900A and digitized at 20 Hz with Axon Digidata1440A and pClamp10. Electrodes contained 3 M KCl and had a resistance of 1–2 megaohms. Drugs (agonists and antagonists) were prepared daily in bath solution. Drug was applied using a Valvelink 8.2 perfusion system (AutoMate Scientific, Berkeley, CA). Atropine (1 μM) was always co-applied for ACh-based recordings to eliminate muscarinic acetylcholine receptor responses. nAChR β3 constructs were tested individually or in batches as they became available to get an estimate of their effect on the function of α6*-nAChRs. Then, for the purpose of comparison, electrophysiological recordings were performed in a given day in a given batch of oocytes following the same order of injections. Hence data points in a figure panel were obtained under similar experimental conditions.

Experimental Controls—Injection of water or empty vector (used as two forms of negative controls) or of cRNA corresponding to one subunit alone or pairwise combinations of nAChR β3, $\beta3^{V9'S}$, $\beta3^{V13'S}$, or other forms of β3 subunits with either an α6 or other forms of α6 or β4 subunit (~7–46 ng of total cRNA) did not result in the expression of functional nAChRs. Current responses to 100 μM nicotine or ACh were less than 5–10 nA (data not shown).

Data Analyses—Raw data were collected and processed in part using pClamp 10.2 (Molecular Devices) and a spreadsheet (Excel, Microsoft, Bellevue, WA) using peak current amplitudes as measures of functional nAChR expression, and results were pooled across experiments (mean ± S.E. for data from at least three oocytes). In some cases, mean peak current amplitudes in response to a single concentration of an agonist were compared across different subunit combinations. However, assessment of true I_{max} values for different nAChR subunit combinations required assessment based on more complete concentration-response relationships in which mean peak current amplitudes at specified ligand concentrations were fit to the Hill equation or its variants using Prism 4 (GraphPad Software, San Diego, CA). F-tests ($p < 0.05$ to define statistical significance) were carried out to compare the best fit values of log molar EC_{50} values across specific nAChR subunit combinations.

There are limitations in the ability to compare levels of functional nAChR expression even though we injected similar amounts of RNA for all constructs. This is because expression levels assessed as peak current amplitudes are affected by batch-to-batch variation in oocytes, time between cRNA injection and recording, and subunit combination-specific parameters, such as open probability (influenced by gating rate constants and rates and extents of desensitization), single channel conductance, assembly efficiency, and efficiency of receptor trafficking to the cell surface (39). We made no attempt to measure or control for subunit combination-specific effects, but whenever preliminary studies revealed possible differences in peak current amplitudes, findings were further confirmed across different subunit combinations using the same batch of oocytes and the same time between cRNA injection and recording (15, 19, 30, 38). Therefore peak current amplitudes shown for representative traces in some figures, pooled data from limited sets of studies, and mean peak current amplitudes across all studies for a given combination of subunits given in tables or figures sometimes differ. However, when we make statements about results comparing ligand potencies and efficacies across subunit combinations, the observations are clear, significant, and in agreement whether for pooled data or for results from smaller sets of studies (one-way analyses of variance followed by Tukey's multiple comparison tests).

RESULTS

Previously (15) we have shown that coexpression of WT nAChR α6 and β2 subunits alone or in combination with β3 or $\beta3^{V9'S}$ subunits in oocytes, all from a single species (human or mouse), did not yield consistent and reproducible current responses to nicotinic agonists. However, under similar experimental conditions, we were able to show that coexpression of mα6 subunits, instead of hα6 subunits, with hβ2 and $h\beta3^{V9'S}$ subunits led to expression of functional hybrid $m\alpha6h\beta2h\beta3^{V9'S}$-nAChRs (15). Also, hybrid mα6hβ4hβ3-nAChRs were fully functional, although there was no function for hα6hβ4hβ3- or mα6mβ4mβ3-nAChRs (15). These studies were carried out by injecting ~1–6 ng of cRNAs for each subunit into oocytes. In continuation of our earlier efforts, in this study, we substituted human β3 subunits for mouse β3 subunits. Initially we injected about ~3.5 ng of cRNAs for each nAChR subunit to express hybrid nAChRs, but later we increased amounts injected to ~23 ng for each subunit to emulate the approach taken by Kuryatov *et al.* (14) to express functional human α6β4*-nAChRs.

Incorporation of nAChR hβ3, $h\beta3^{V9'S}$, or $h\beta3^{V13'S}$ Subunits Potentiates mα6mβ4-nAChR Function*—Coexpression with WT hβ3 subunits significantly ($p < 0.05$) potentiated ACh- or nicotine-induced current responses of mα6mβ4-nAChRs (Fig. 2 and Table 2). Also, coexpression with nAChR $h\beta3^{V9'S}$ or $h\beta3^{V13'S}$ subunits increased ($p < 0.05$) the current responses further (Fig. 2 and Table 2). The increase in agonist sensitivities and in peak current amplitudes indicate that WT hβ3 subunits incorporate into at least some complexes containing mα6 and mβ4 subunits and these effects are most likely due to higher levels of functional receptor expression. Moreover, whereas not all oocytes expressing mα6 and mβ4 subunits yield functional

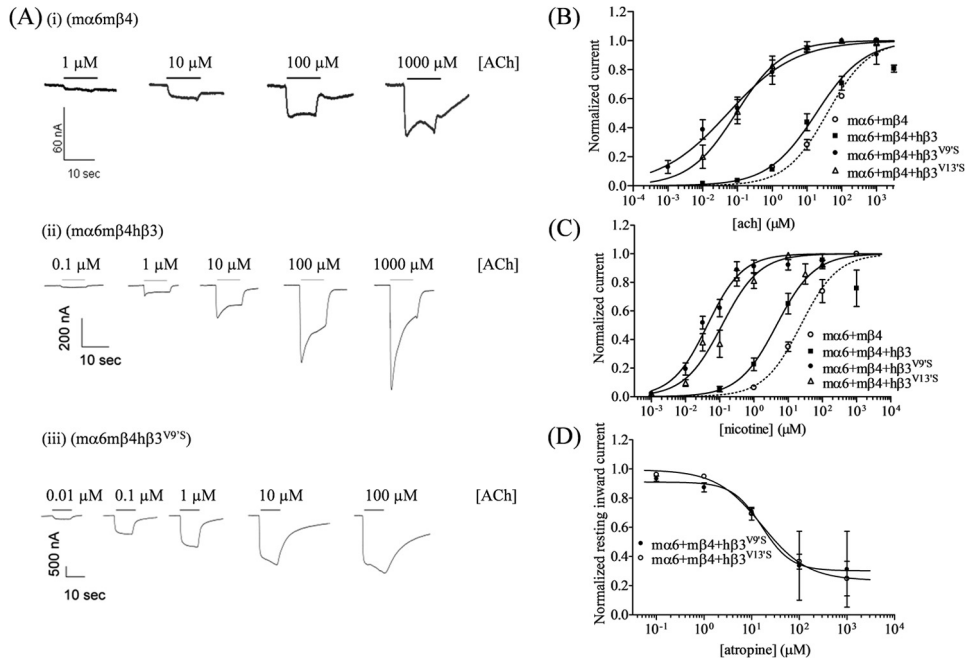

FIGURE 2. **Concentration-dependent effects of agonist exposure on current responses in oocytes expressing mα6mβ4*-nAChRs.** *A*, representative traces are shown for inward currents in oocytes held at −70 mV responding to application at the indicated concentrations of ACh (shown with the duration of agonist exposure as *black bars* above the traces) and expressing nAChR mα6 and mβ4 subunits alone (*panel i*) or in the additional presence of wild-type hβ3 (*panel ii*) or hβ3$^{V9'S}$ (*panel iii*) subunits. *Calibration bars* are for 60-, 200-, or 500-nA currents (*vertical*) and 10 s (*horizontal*). Results for these and other studies averaged across experiments were used to produce agonist- or antagonist-induced concentration-response curves (*ordinate*, mean normalized current ±S.E. (*error bars*); *abscissa*, ligand concentration in log μM) for responses to ACh (*B*), nicotine (*C*), or atropine (*D*) for oocytes expressing nAChR mα6 and mβ4 subunits alone (○) or in the additional presence of hβ3 (■), hβ3$^{V9'S}$ (●), or hβ3$^{V13'S}$ (△) subunits as indicated. Leftward shifts in agonist concentration-response curves are evident for functional nAChR containing hβ3, hβ3$^{V9'S}$, or hβ3$^{V13'S}$ subunits ($p < 0.0001$; ~2-, ~717-, and ~418-fold, respectively, for ACh EC_{50} values and ~6-, ~605-, and 217-fold, respectively, for nicotine EC_{50} values relative to the respective agonist EC_{50} values for activation of mα6mβ4-nAChR function). See Table 2 for parameters.

TABLE 2

Parameters for drug action at hybrid hα6hβ4*- or mα6mβ4*-nAChRs

Potencies (micromolar EC_{50} or IC_{50} values with 95% confidence intervals (CI)), Hill coefficients (n_H ± S.E.), mean ± S.E. efficacies (I_{max} in nA), and concentrations (conc.) where maximal peak current amplitudes (I_{max}) are achieved (μM) are provided for the indicated agonist (ACh or nicotine) or antagonist (atropine) acting at nAChR composed of the indicated subunits derived from the specified species and from the indicated number of independent experiments (*n*) based on studies as shown in Fig. 2. ↑ indicates a significant ($p < 0.05$) increase in potency or efficacy of the specified agonist at the indicated nAChR subtype relative to nAChR upon expression in the presence of the indicated wild-type or mutant β3 subunit instead of in the absence of a β3 subunit, ▲ indicates a significant increase in specified agonist potency or efficacy at the indicated nAChR subtype upon substitution of a mutant for a wild-type β3 subunit relative to nAChR containing the same subunits in the presence of wild-type β3 subunits, and △ or ▽ indicates a significant increase or decrease, respectively, in potency or efficacy of the specified agonist or antagonist at the indicated nAChR subtype containing β3$^{V13'S}$ instead of β3$^{V9'S}$ subunits.

Drug	nAChR subunit combinations	Potency			Peak response		
		n	EC_{50} or IC_{50} (95% CI)	n_H ± S.E.	*n*	Mean I_{max} ±S.E.	I_{max} conc.
			μM			nA	μM
ACh	mα6 + mβ4[a]	3	38 (25–58)	0.72 ± 0.09	3	65 ± 25	1000
	mα6 + mβ4 + hβ3	4	18 (12–28) ↑	0.62 ± 0.07	4	358 ± 128 ↑	100
	mα6 + mβ4 + hβ3$^{V9'S}$	4	0.05 (0.03–0.11) ↑▲	0.45 ± 0.07	3	3379 ± 189 ↑▲	100 ↑▲
	mα6 + mβ4 + hβ3$^{V13'S}$	4	0.09 (0.05–0.16) ↑▲	0.64 ± 0.1	4	2989 ± 43 ↑▲	100 ↑▲
Nicotine	mα6 + mβ4[a]	3	24 (14–50)	0.65 ± 0.13	5	27 ± 7	1000
	mα6 + mβ4 + hβ3	4	4.5 (2.5–8.3) ↑	0.78 ± 0.16	4	212 ± 5 ↑	100 ↑
	mα6 + mβ4 + hβ3$^{V9'S}$	6	0.04 (0.03–0.06) ↑▲	0.84 ± 0.10	7	2884 ± 333 ↑▲	10 ↑▲
	mα6 + mβ4 + hβ3$^{V13'S}$	7	0.12 (0.08–0.17) ↑▲▽	0.79 ± 0.1	8	2783 ± 622 ↑▲	10 ↑▲
Atropine	mα6 + mβ4 + hβ3$^{V9'S}$	3	16 (1–241)	−1.40 ± 2.4	3	140.8 ± 13.44	1000
	mα6 + mβ4 + hβ3$^{V13'S}$	3	17 (4.8–58)	−0.90 ± 0.46	3	512.6 ± 28.87 △	1000

[a] Data from Ref. 15.

responses to nicotinic agonists, almost all oocytes expressing nAChR mα6, mβ4, and hβ3 subunits produced functional responses, suggesting that nAChR hβ3 subunits facilitate formation of functional, trinary (containing three kinds of subunits) nAChRs.

Spontaneously Opening mα6mβ4hβ3$^{V9'S}$- or mα6mβ4hβ3$^{V13'S}$-nAChRs Are Sensitive to Blockade by Atropine—Atropine (1 μM) was always co-applied for ACh-based recordings to eliminate muscarinic acetylcholine receptor responses. Because atropine at higher concentrations also can interact with different nAChR subtypes (15, 40, 41), initially as a simple control, we assessed the effects of atropine at different concentrations alone on all receptor combinations studied. Atropine alone did not produce any effect when assessed using oocytes expressing any combination of WT nAChR subunits (data not shown), but it reversibly produced outward currents when applied to oocytes expressing receptors containing β3$^{V9'S}$ or β3$^{V13'S}$ subunits. The concentration-dependent effects of atropine were

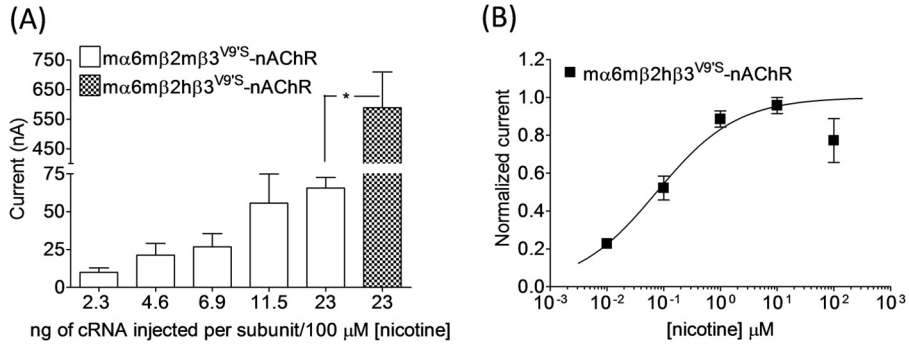

FIGURE 3. **Effects of agonist exposure on current responses in oocytes expressing mα6mβ2(mβ3$^{V9'S}$ or hβ3$^{V9'S}$)-nAChRs.** *A*, current responses (mean ± S.E. (*error bars*); nA) to 100 μM nicotine obtained on the 5th day after injection from oocytes (n = 3–6) voltage-clamped at −70 mV and expressing mα6mβ2mβ3$^{V9'S}$ or mα6mβ2hβ$^{V9'}$-nAChRs. Oocytes were injected with the indicated amount (ng) of cRNA for each subunit. *B*, concentration-response curve for responses to nicotine (*ordinate*, mean normalized inward current ±S.E. (*error bars*); *abscissa*, ligand concentration in log μM) for oocytes expressing mα6mβ2hβ3$^{V9'S}$-nAChRs. *, $p < 0.05$.

defined in terms of IC_{50} values for half-maximal blockade of spontaneous function, which for mα6mβ4hβ3$^{V9'S}$- and mα6mβ4hβ3$^{V13'S}$-nAChRs were 16 and 17 μM, respectively (Fig. 2 and Table 2). It is estimated, based on comparisons of atropine-induced outward current peak amplitudes with the sum of those currents plus inward currents induced by fully efficacious concentrations of nicotine or ACh, that more than 4–16% of these receptors are spontaneously open at any one time.

Function of mα6mβ2-nAChRs Is Potentiated by Coexpression with nAChR mβ3$^{V9'S}$ Subunits and Is Yet Higher upon Coexpression with hβ3$^{V9'S}$ Instead of mβ3$^{V9'S}$ Subunits*—Coexpression of hβ3 or hβ3$^{V9'S}$ subunits in oocytes also expressing mα6 and mβ2 subunits did not lead to reproducible current responses to ACh or nicotine whenever they were expressed using ~3 ng of cRNA for each subunit (data not shown). We decided to inject higher amounts of cRNA for each subunit (similar to the approach taken by Kuryatov *et al.* (14) to express hα6hβ4- or hα6hβ4hβ3-nAChRs) to see whether that would influence the functional expression of mα6mβ2*-nAChRs. Current responses to nicotine from oocytes expressing mα6mβ2mβ3$^{V9'S}$-nAChRs increased with injection of increased amounts of cRNA for each subunit (Fig. 3). However, at the largest amount of cRNA for each subunit injected (~23 ng), there was no functional expression of mα6mβ2mβ3- or mα6mβ2hβ3-nAChRs. Nonetheless, oocytes expressing mα6mβ2hβ3$^{V9'S}$-nAChRs yielded higher peak current responses (589 ± 121 *versus* 66 ± 7 nA; ~9-fold; $p < 0.05$) than those expressing mα6mβ2mβ3$^{V9'S}$-nAChRs (Fig. 3). Oocytes expressing mα6mβ2hβ3$^{V9'S}$-nAChRs, but not mα6mβ2mβ3$^{V9'S}$-nAChRs, cultured for prolonged times produced some outward reversible currents in response to atropine (data not shown). The EC_{50} value for nicotine for activation of mα6mβ2hβ3$^{V9'S}$-nAChRs is 0.08 μM.

Incorporation of Chimeric Mouse/Human β3 Subunits into Mouse α6β2- and α6β4*-nAChRs*—We extended our studies to work using chimeric mouse/human nAChR β3 subunits to understand the molecular bases for the differential effect of mβ3 and hβ3 subunits on mα6*-nAChR function. We first constructed the BglII site-based nAChR chimeric subunit mβ3(1–329)/hβ3(324–458). We injected ~23 ng of cRNA for each subunit as we did for expression of mα6mβ2(mβ3$^{V9'S}$ or hβ3$^{V9'S}$)-nAChRs to express mα6mβ4-, mα6mβ4mβ3-, mα6mβ4hβ3-, or mα6mβ4mβ3(1–329)/hβ3(324–458)-nAChRs. Initial assessments indicated that all these nAChRs were functional, but the current responses from oocytes expressing mα6mβ4mβ3(1–329)/hβ3(324–458)-nAChRs were similar to those from oocytes expressing mα6mβ4-nAChRs and lower than those elicited from oocytes expressing mα6mβ4hβ3-nAChRs (see Fig. 4*B*). Coexpression of this chimeric subunit with mα6 and mβ2 subunits did not produce any detectable functional nAChR. These results prompted us to construct two additional chimeras that either increased or reduced the length of the hβ3 subunit contribution to mouse/human β3 subunit chimeras. This led to construction of chimeric mβ3(1–187)/hβ3(182–458) (SalI restriction site-based) and mβ3(1–375)/hβ3(370–458) (BsiWI restriction site-based) subunits. All three chimeras were assessed in parallel for their effects on mα6mβ2*- or mα6mβ4*-nAChRs.

Coexpression of chimeric mouse/human nAChR subunits (*i.e.* mβ3(1–187)/hβ3(182–458), mβ3(1–329)/hβ3(324–458), or mβ3(1–375)/hβ3(370–458)) with nAChR mα6 and mβ2 subunits in oocytes did not result in detectable nAChR function (data not shown). However, these chimeric subunits coexpressed with mα6 and mβ4 subunits yielded minimally functional nAChRs. Results indicated that peak current responses of mα6mβ4[mβ3(1–187)/hβ3(182–458)]-, mα6mβ4[mβ3(1–329)/hβ3(324–458)]-, or mα6mβ4[mβ3(1–375)/hβ3(370–458)]-nAChRs are similar ($p > 0.05$) to those of mα6mβ4- (50 ± 13 nA; 1000 μM nicotine) or mα6mβ4mβ3-nAChRs (85 ± 15 nA; 100 μM nicotine) but lower ($p < 0.05$) than those of mα6mβ4hβ3-nAChRs (410 ± 88 nA; 100 μM nicotine) (Fig. 4*B*).

Incorporation of Gain-of-function Chimeric Mouse/Human nAChR β3 Subunits into Mouse α6β2- and α6β4*-nAChRs*—To evaluate whether the chimeric nAChR mβ3/hβ3 subunits are truly participating in mα6*-nAChR formation, we assessed the incorporation of gain-of-function mβ3(1–187)/hβ3(182–458)$^{V9'S}$, mβ3(1–329)$^{V9'S}$/hβ3(324–458), or mβ3(1–375)$^{V9'S}$/hβ3(370–458) subunits into mα6mβ2*- and mα6mβ4*-nAChRs. Coexpression of these gain-of-function chimeric nAChR subunits with mα6 and mβ2 subunits in oocytes resulted in the production of functional nAChRs (Fig. 4*A*). Current responses from oocytes expressing chimeric mα6mβ2*-nAChRs progressively decreased when coexpressed with chi-

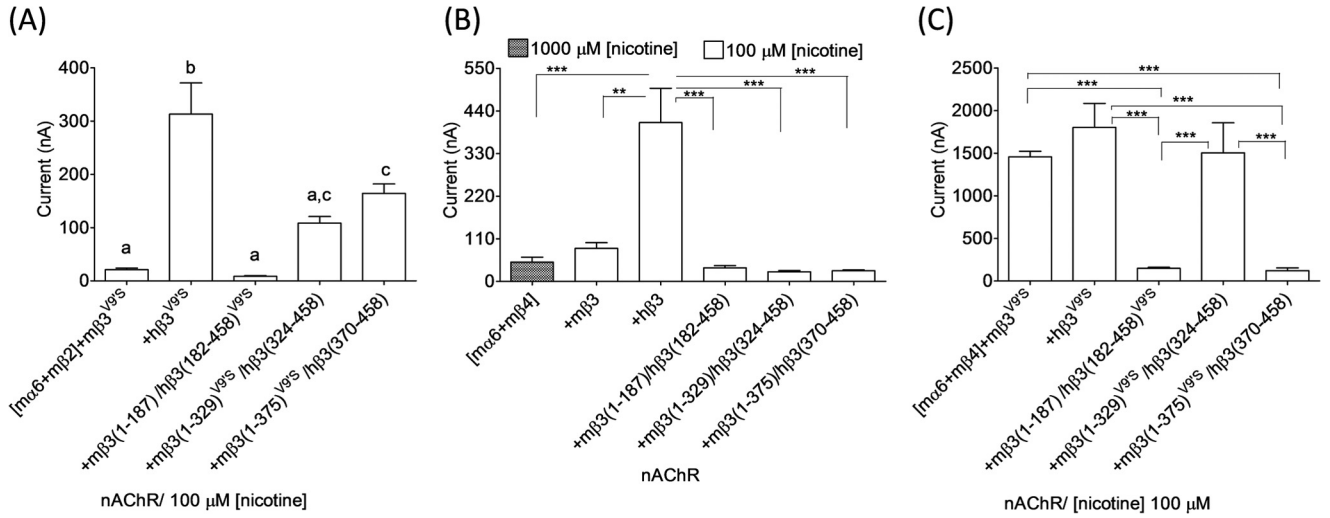

FIGURE 4. **Effects of chimeric mouse/human or gain-of-function chimeric mouse/human nAChR β3 subunits on functional responsiveness of mα6*-nAChRs.** *A–C*, mean ± S.E. (*error bars*) peak inward current responses upon exposure to 100 or 1000 μM nicotine (5-s exposure; *ordinate*) from oocytes (n = 3–10) voltage-clamped at −70 mV and heterologously expressing mα6mβ2*- (*A*) or mα6mβ4*-nAChRs (*B* and *C*) in the presence of the indicated chimeric nAChR β3 subunits. Note that mα6mβ4-nAChRs reach I_{max} at 1000 μM nicotine. The largest amplitude responses to nicotine were observed when hβ3 or hβ3$^{V9'S}$ subunits were present in mα6mhβ2*- or mα6mhβ4*-nAChRs. Current responses were compared using one-way analyses of variance with Tukey's post hoc comparison. Groups with different *letters* (*a*, *b*, and *c*) are significantly ($p < 0.05$) different. **, $p < 0.01$; ***, $p < 0.001$.

meric β3 subunits containing shorter N-terminal segments from the mouse β3 subunit. For example, mα6mβ2[mβ3(1–187)/hβ3(182–458)$^{V9'S}$]-nAChRs were least responsive to nicotine. This suggested that a combination of mβ3 subunit domains and residues contributes to impeded functional expression of mα6mβ2*-nAChRs.

Incorporation of mβ3(1–187)/hβ3(182–458)^{V273S}, mβ3(1–329)^{V279S}/hβ3(324–458), or mβ3(1–375)^{V279S}/hβ3(370–458) subunits into mα6mβ4-nAChRs yielded functional nAChRs (Fig. 4*C*). Peak current responses from oocytes expressing mα6mβ4[mβ3(1–329)^{V279S}/hβ3(324–458)]-nAChRs (1505 ± 353 nA) were similar ($p > 0.05$) to those of mα6mβ4mβ3^{V279S}- or mα6mβ4hβ3^{V273S}-nAChRs. However, oocytes expressing mα6mβ4[mβ3(1–187)/hβ3(182–458)^{V273S}]- (148 ± 13 nA) or mα6mβ4[mβ3(1–375)^{V279S}/hβ3(370–458)]-nAChRs (122 ± 33 nA) yielded much lower ($p < 0.001$) peak current responses than those expressing either mα6mβ4mβ3^{V279S}- or mα6mβ4hβ3^{V273S}-nAChRs. Although the presence of hβ3 subunit residues from TM III through the large, second cytoplasmic domain to the C terminus seems somehow to quell such an effect, this again suggested that a combination of mβ3 subunit domains and residues contributes to reduced functional expression of mα6mβ4*-nAChRs. However, strongest implications were that the extracellular N-terminal domain was involved.

N-terminal AA Residues in the nAChR mβ3 Subunit That Influence the Function of Mouse α6β2- and α6β4*-nAChRs*—Because effects on mα6mβ2*- and mα6mβ4*-nAChR function were most extreme in chimeras containing extracellular N-terminal domains from the mβ3 subunit, we focused on this region and on residues that differ between hβ3 and mβ3 subunits. For all nAChR subunits, there is a "primary" or (+) face and a "complementary" or (−) face where subunit extracellular N-terminal domains interact, forming a subunit interface. Interface interactions are critical for subunits to form dimers and for dimers to join with a single subunit to close the pentameric assembly. Interfaces involving the primary face of specific α subunits and the complementary face of specific β subunits also are known to contain agonist binding pockets, occupancy of which leads to channel opening and where competitive antagonists also bind to affect function (the α subunit was designated as that providing the primary face because it was initially thought that agonist binding sites resided solely within α subunits). nAChR biologists have identified several loops at turns in β-strands that criss-cross subunit extracellular domains as in a woven basket. So-called loop β2-β3 (named so because the loop is formed at the tip of a turn between β strands β2 and β3) and loops D, E, and F are evident from modeling and structural studies to be on the complementary face of a given subunit, whereas loops A, B, and C are on the primary face. Loops A–F appear to be engaged in ligand recognition. For site-directed mutagenesis studies, we focused on some of the very few residues that differ between hβ3 and mβ3 subunits, AAs Gln^{94}, Glu^{101}, and Asn^{107} in the β2-β3 loop; AAs Ser^{144} and Ser^{148} in putative loop E, and AAs Glu^{221} and Phe^{223} in putative loop C, to determine roles in functional expression of mα6mβ2*- and mα6mβ4*-nAChRs (Fig. 1*A*). Residues in the nAChR mβ3 subunit were mutated to their counterparts in the nAChR hβ3 subunit alone or in specific combinations (*i.e.* mβ3(Q94H), mβ3(E101D), mβ3(N107H), mβ3(Q94H/E101D), mβ3(Q94H/N107H), mβ3(S144N/S148V), mβ3(E221D), and mβ3(E221D/F223V)) (Fig. 5).

AA Substitutions in the β2-β3 Loop of nAChR mβ3 Subunit Influence the Current Responses of mα6mβ2- or mα6mβ4*-nAChRs*—Coexpression of nAChR mβ3 subunit point mutants (Q94H, E101D, or N107H) or double mutants (Q94H/E101D or Q94H/N107H) in oocytes with mα6 and mβ2 subunits did not lead to production of functional nAChR. However, these mutant subunits harboring the V9′S mutation in their respective TM II domains (*i.e.* mβ3(Q94H)$^{V9'S}$, mβ3(E101D)$^{V9'S}$, mβ3(N107H)$^{V9'S}$, mβ3(Q94H/E101D)$^{V9'S}$, or mβ3(Q94H/N107H)$^{V9'S}$) upon coexpression with mα6 and

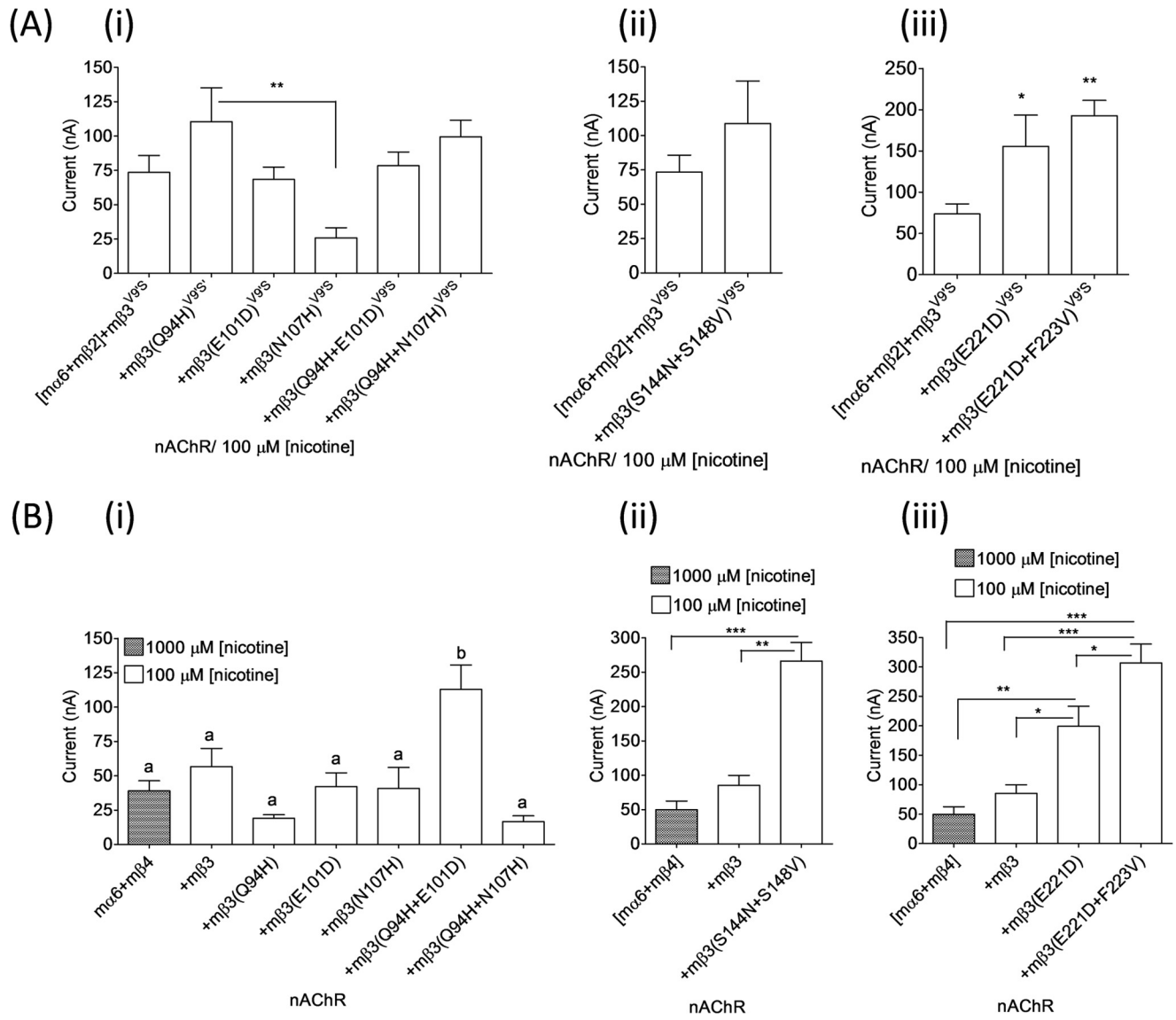

FIGURE 5. **Effects of nAChR mβ3 subunit amino acid substitutions on the current responses of mα6*-nAChRs.** *A* and *B*, current responses (mean ± S.E. (*error bars*)) from oocytes ($n = 3–6$) (voltage-clamped at −70 mV) responding to the application of 100 or 1000 μM nicotine (5-s exposure; *ordinate*) were measured from mα6mβ2*- (*A*) or mα6mβ4*-nAChRs (*B*) harboring WT, mutant, or gain-of-function mβ3-, mβ3(Q94H)-, mβ3(E101D)-, mβ3(E107H)-, mβ3(Q94H/E101D)-, or mβ3(Q94H/N107H)-nAChR subunits (*panel i*); WT, mutant, or gain-of-function mβ3- or mβ3(S144N/S148V)-nAChR subunits (*panel ii*); or WT, mutant, or gain-of-function mβ3-, mβ3(E221D)-, or mβ3(E221D/F223V)-nAChR subunits (*panel iii*). Current responses were compared using Student's *t* test (two-tailed) or one-way analyses of variance (with Tukey's post hoc comparison). Groups with different *letters* (*a* and *b*) are significantly ($p < 0.05$) different. *, $p < 0.05$; **, $p < 0.01$; ***, $p < 0.001$.

mβ2 subunits in oocytes and responding to application of 100 μM nicotine produced peak current responses of 110 ± 25, 68 ± 9, 26 ± 7, 78 ± 10, or 99 ± 12 nA, respectively (Fig. 5*A*, *panel i*). The peak current responses of mα6mβ2[mβ3(Q94H)$^{V9'S}$]-, mα6mβ2[mβ3(E101D)$^{V9'S}$]-, mα6mβ2[mβ3(N107H)$^{V9'S}$]-, mα6mβ2[mβ3(Q94H/E101D)$^{V9'S}$]-, or mα6mβ2[mβ3(Q94H/N107H)$^{V9'S}$]-nAChRs did not differ ($p < 0.05$) from those of mα6mβ2mβ3$^{V9'S}$-nAChRs (73 ± 12 nA).

Oocytes expressing mα6 and mβ4 subunits alone or in the additional presence of mβ3(Q94H), mβ3(E101D), mβ3(N107H), mβ3(Q94H/E101D), or mβ3(Q94H/N107H) subunits produced functional nAChRs (Fig. 5*B*, *panel i*). Peak current responses of mα6mβ4mβ3-nAChRs (57 ± 13 *versus* 113 ± 18 nA) were increased (~2-fold; $p < 0.05$) as a result of Q94H/N107H double substitution in the nAChR mβ3 subunit. Also, the current responses of mα6mβ4mβ3(Q94H/N107H)-nAChRs were higher (~3-fold; $p < 0.05$) than those of mα6mβ4-nAChRs (39 ± 7 nA).

AA Substitutions in Loop E of the nAChR mβ3 Subunit Influence the Function of mα6mβ2- or mα6mβ4*-nAChRs*—Coexpression of gain-of-function nAChR mβ3(S144N/S148V)$^{V9'S}$ subunits, but not nAChR mβ3(S144N/S148V) subunits, in oocytes with mα6 and mβ2 subunits resulted in production of functional nAChRs. Current responses of mα6mβ2[mβ3(S144N/S148V)$^{V9'S}$]-nAChRs to 100 μM nicotine (109 ± 31 nA) were not different ($p < 0.05$) from those of mα6mβ2mβ3$^{V9'S}$-nAChRs (73 ± 12 nA) (Fig. 5*Aii*). Peak current responses of mα6mβ4mβ3-nAChRs were increased (266 ± 27 *versus* 85 ± 15 nA; ~2.5-fold; $p < 0.05$) as a result of the S144N/S148V double mutation in the nAChR mβ3 subunit (Fig. 5*Bii*). EC_{50} values for nicotine at mα6mβ4hβ3-, mα6mβ4mβ3-, and

mα6mβ4mβ3(S144V/S148V)-nAChRs (*i.e.* 4.5, 6.6, and 10 μM, respectively; Fig. 6 and Table 3) were essentially the same ($p > 0.05$).

AA Substitutions in Loop C of in the nAChR mβ3 Subunit Influence the Function of mα6mβ2 or mα6mβ4*-nAChRs*—Oocytes expressing mα6mβ2[mβ3(E221D)$^{V9'S}$]- (155 ± 38 nA) or mα6mβ2[mβ3(E221D/F223V)$^{V9'S}$] (193 ± 18 nA)-nAChRs elicited higher (~2–3-fold; $p < 0.05$) peak currents in response to 100 μM nicotine than those expressing mα6mβ2mβ3$^{V9'S}$-nAChRs (73 ± 12 nA; Fig. 5*Aiii*). However, coexpression of nAChR mβ3(E221D) or mβ3(E221D/F223V) subunits in oocytes with mα6 and mβ2 subunits did not result in expression of functional nAChR. Substitution of nAChR mβ3(E221D) (199 ± 34 nA; ~2-fold) or mβ3(E221D/F223V) (307 ± 32 nA; ~6-fold) subunits for mβ3 subunit increased ($p < 0.05$) the current responses of mα6mβ4mβ3-nAChRs (85 ± 15 nA (Fig. 5*Biii*)). However, EC_{50} values for nicotine at mα6mβ4mβ3- (6.6 μM) or mα6mβ4hβ3 (4.5 μM)-nAChRs were not altered ($p > 0.05$) when mβ3(E221D) (4 μM) or mβ3(E221D/F223V) (6.5 μM) subunits were substituted for mβ3 subunits (Fig. 6 and Table 3).

AA Substitutions in Loop C of nAChR mβ3 Subunit Also Influence Function of mα6$^{(L9'S\ or\ V13'S)}$mβ2-nAChRs*—Previously, we could not detect functional expression of mα6$^{L9'S}$mβ2- or mα6$^{V13'S}$mβ2-nAChRs or of mα6$^{L9'S}$mβ2mβ3- or mα6$^{V13'S}$mβ2hβ3-nAChRs in oocytes (38). Upon increasing the amount of cRNA injected for each subunit to ~23 ng, there was emergence of functional mα6$^{(L9'S\ or\ V13'S)}$mβ2mβ3-nAChRs, but not mα6$^{(L9'S\ or\ V13'S)}$mβ2-nAChRs, in oocytes. However, nicotine-elicited (100 μM) peak current responses from oocytes expressing mα6$^{V13'S}$mβ2mβ3-nAChRs were higher (70 ± 18 *versus* 9 ± 1 nA; ~8-fold; $p < 0.05$) than those expressing mα6$^{L9'S}$mβ2mβ3-nAChRs (Fig. 7).

We also assessed whether substitutions of AA residues in loop C of the nAChR mβ3 subunit would increase the peak current responses of mα6$^{L9'S}$mβ2*- or mα6$^{V13'S}$mβ2*-nAChRs. Nicotine-elicited (100 μM) peak current responses from oocytes expressing mα6$^{L9'S}$mβ2mβ3- (9 ± 1 *versus* 17 ± 2 nA) or mα6$^{V13'S}$mβ2mβ3 (70 ± 18 *versus* 170 ± 28 nA)-nAChRs were increased ($p < 0.05$) as a result of E221D/F223V substitution in the nAChR mβ3 subunit. Also, oocytes expressing mα6$^{V13'S}$mβ2mβ3(E221D)-nAChRs (162 ± 32 nA) yielded higher peak current ($p < 0.05$) in response to 100 μM nicotine

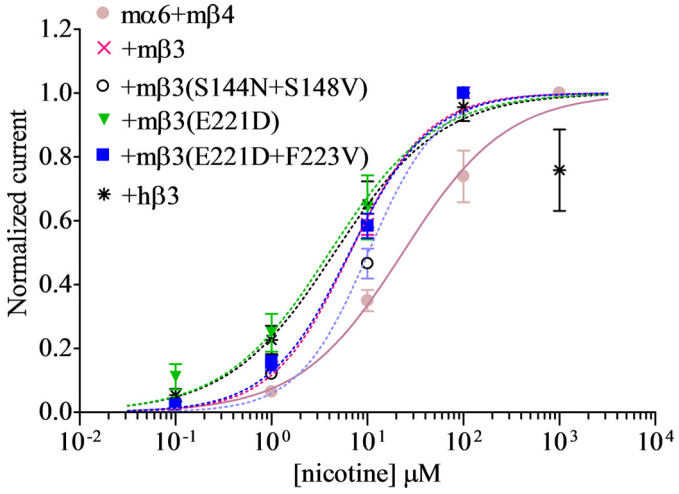

FIGURE 6. **Effects of nAChR mβ3 subunit amino acid substitutions on nicotine sensitivities of mα6mβ4*-nAChRs.** Concentration-response curves (*ordinate*, mean normalized current ±S.E. (*error bars*); *abscissa*, ligand concentration in log μM) are shown for responses to nicotine for oocytes expressing nAChR mα6 and mβ4 subunits alone (●) or in the additional presence of hβ3 (*), mβ3 (×), hβ3(S144N/S148V) (○), hβ3(E221D) (▼), or hβ3(E221D/F223V) (■) subunits as indicated. Leftward shifts in agonist concentration-response curves are evident for functional nAChRs containing hβ3, mβ3, hβ3(S144N/S148V), hβ3(E221D), hβ3(E221D/F223V), or hβ3(E347Q/R361K) subunits. See Table 3 for parameters.

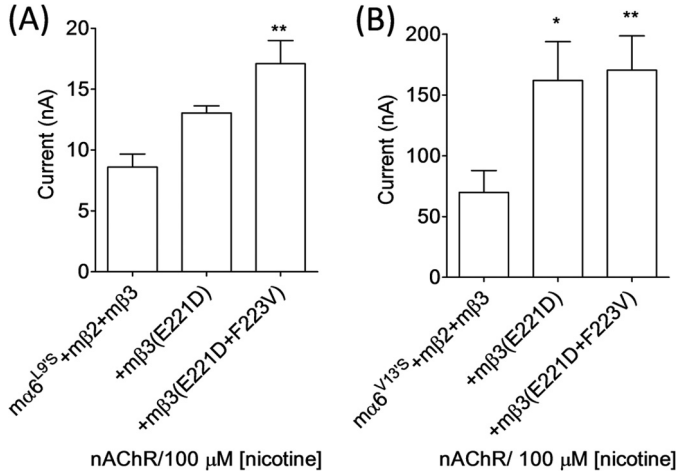

FIGURE 7. **Effects of nAChR mβ3 subunit loop C amino acid substitutions on functional responsiveness of mα6$^{(L9'S\ or\ V13'S)}$mβ2*-nAChRs.** Mean ± S.E. (*error bars*) peak inward current responses upon exposure to 100 μM nicotine (5-s exposure; *ordinate*) were measured from oocytes ($n = 3–6$) voltage-clamped at −70 mV and heterologously expressing mα6$^{L9'S}$, mβ2- plus mβ3-, mβ3(E221D)-, or mβ3(E221D/F223V)- (*A*) or mα6$^{V13'S}$-, mβ2- plus mβ3-, mβ3(E221D)-, or mβ3(E221D/F223V)-nAChR subunits (*B*). Current responses were compared using one-way analyses of variance (with Tukey's post hoc comparison). *, $p < 0.05$; **, $p < 0.01$.

TABLE 3

Parameters for nicotine action at nAChRs containing mα6 and mβ3 mutant subunits

Potencies (micromolar EC_{50} values with 95% confidence intervals (CI)), Hill coefficients (n_H ± S.E.), mean ± S.E. efficacies (I_{max} in nA), and concentrations (conc.) where maximal peak current amplitudes (I_{max}) are achieved (μM) are provided for nicotine acting at mouse nAChR composed of the indicated subunits and from the indicated number of independent experiments (n) based on studies as shown in Fig. 6. ↑ indicates a significant ($p < 0.05$) increase in the indicated parameter at the indicated nAChR subtype relative to wild-type mα6mβ4-nAChR, and ▲ indicates a significant ($p < 0.05$) increase in the indicated parameter at the indicated nAChR subtype relative to wild-type mα6mβ4mβ3-nAChR.

nAChR subunit combinations	n	Potency		Peak response	
		EC_{50} (95% CI)	n_H ± S.E.	Mean I_{max} ±S.E.	I_{max} conc.
		μM		nA	μM
mα6 + mβ4	6	23 (15–37)	0.8 ± 0.13	50 ± 13	1000
mα6 + mβ4 + mβ3	3	6.6 (5.1–8.5) ↑	1.1 ± 0.12	85 ± 15	100 ↑
mα6 + mβ4 + mβ3(S144N/S148V)	5	10 (8.2–13) ↑	1.2 ± 0.18	266 ± 27 ↑▲	100 ↑
mα6 + mβ4 + mβ3(E221D)	5	4 (2.3–7.2) ↑	0.8 ± 0.18	199 ± 34 ↑▲	100 ↑
mα6 + mβ4 + mβ3(E221D/F223V)	5	6.5 (5.1–8.2) ↑	1 ± 0.11	307 ± 32 ↑▲	100 ↑

than those expressing mα6$^{V13'S}$mβ2mβ3-nAChRs. These results confirm the previous findings that TM II 13′ valine-to-serine mutations in the mα6 subunit are more capable of attributing gain of function to mα6*-nAChRs than the TM II 9′ leucine-to-serine mutation (38).

DISCUSSION

Functional heterologous expression of human or mouse α6*-nAChRs has been difficult. Various approaches have been undertaken to circumvent this situation for human α6*-nAChRs (14, 15, 19, 22, 31, 38, 42). There is hardly any focus on heterologous expression of functional mouse α6*-nAChRs, although they are known to be physiologically important (3, 8, 10, 12, 43–45). Our initial studies, using ~1–6 ng of cRNA for each subunit, indicated that mouse α6β4-nAChRs expressed in oocytes are minimally functional (15). Although there was no emergence of functional mouse α6β4β3-nAChRs in oocytes, mouse α6β4β3$^{V9'S}$-nAChRs in oocytes were highly functional (15). Functional mα6mβ2-, mα6mβ2mβ3-, or mα6mβ2mβ3$^{V9'S}$-nAChRs or mα6$^{L9'S}$mβ2-, mα6$^{L9'S}$mβ2mβ3-, mα6$^{V13'S}$mβ2-, or mα6$^{V13'S}$mβ2mβ3-nAChRs also were not detected in oocytes (15, 38). In continuation of these studies, here we used various approaches to produce or enhance the functional expression of mouse α6*-nAChRs.

We noticed that upon substitution of nAChR hβ3 subunits for nAChR mβ3 subunits highly functional hybrid mα6mβ4hβ3-nAChRs were produced in oocytes. We also noticed that functional mα6mβ4mβ3-nAChRs were formed in oocytes when they were expressed using an injection of relatively larger amounts of cRNAs (~23 ng) for each subunit. The peak current responses of these mα6mβ4mβ3-nAChRs were nonetheless severalfold lower than those of hybrid mα6mβ4hβ3-nAChRs. Similar to previous observations (15), whether using relatively lower or higher amounts of injected cRNA for each subunit, functional mα6mβ2-, mα6mβ2mβ3-, or mα6mβ2hβ3-nAChRs were not detected in oocytes. However, upon increasing the amount of cRNA injected for each subunit, minimally functional mα6mβ2mβ3$^{V9'S}$- or robustly functional mα6mβ2hβ3$^{V9'S}$-nAChRs emerged on cell surfaces. Additionally, mα6mβ4*-nAChRs harboring hβ3$^{V9'S}$ or hβ3$^{V13'S}$ subunits showed gain of function similar to those of mα6mβ4mβ3$^{V9'S}$- or mα6mβ4mβ3$^{V13'S}$-nAChRs (15). Therefore, incorporation of hβ3 or mβ3 subunits into mα6mβ4*-nAChRs is evident because it had a potentiation effect. These results also suggest that these WT β3 subunits must be facilitating assembly of functional receptors. Potentiation of agonist sensitivity and levels of functional responses also indicate that there was incorporation of mutant hβ3$^{V9'S}$ or mβ3$^{V9'S}$ subunits into mα6mβ4*- or mα6mβ2*-nAChRs with further facilitation of functional receptor expression, increased frequency of agonist-gated channel opening, or both. These results also are indicative of efficient incorporation of hβ3 subunits, but not that of mβ3 subunits, into assemblies of mα6 and mβ4 subunits or of mα6 and mβ2 subunits.

Our results confirm that trinary complexes involving mα6 plus mβ2 or mα6 plus mβ4 subunits are formed. The observation that functional mα6mβ4*-nAChRs, but not mα6mβ2*-nAChRs, were formed whenever oocytes were injected with higher amount of cRNAs is consistent with such observations made in studies of expression of human α6*-nAChRs in oocytes (14). We also extended this strategy to ensure expression of functional mα6mβ2mβ3$^{V9'S}$- or mα6mβ2hβ3$^{V9'S}$-nAChRs. The need for elevated subunit abundance in oocytes for formation of cell surface, functional α6*-nAChRs is in contrast to the relative ease of expression of functional WT α2β4-, α3β2-, α3β4-, α4β2-, or α4β4-nAChRs or hybrid mα6hβ4hβ3- or mα6hβ2hβ3$^{V9'S}$-nAChRs in oocytes using ~1–2 ng of cRNAs for each subunit (27, 30). This also suggests that differences in features or AA sequence between mβ3 and hβ3 subunits accounts for increased efficiency of subunit assembly to closure of pentameric and functional mα6*-nAChRs.

Transmembrane II 9′ or 13′ valine-to-serine mutants of hβ3 or mβ3 ((hβ3 or mβ3)$^{(V9'S\ or\ V13'S)}$) subunits whenever coexpressed with mα6mβ4*-nAChRs almost always yielded oocytes giving apparently outward current responses to atropine, indicating integration of β3 subunits into mα6mβ4*-nAChRs. This also indicates that these channels are opening spontaneously, a feature commonly seen for receptors of the ligand-gated ion channel family containing gain-of-function mutations (TM II V9′S or V13′S) (15, 19, 38, 46). Effects of atropine at high concentrations reflect its open channel blocking ability, which is seen for oocytes expressing mα6mβ2hβ3$^{V9'S}$-nAChRs but not mα6mβ2mβ3$^{V9'S}$-nAChRs (data not shown).

Differences in amino acid composition between hβ3 and mβ3 subunit extracellular N-terminal and second cytoplasmic loop regions (*e.g.* as opposed to their nearly identical transmembrane domains) that influence effects on α6*-nAChR function were revealed based on studies of chimeric nAChR mouse/human β3 subunits or their gain-of-function variants. The involvement of the NTD of β3 subunits in these effects echoes previous findings that the NTD of hα6 subunits influences assembly and function of human α6β3*-nAChRs (15, 19, 38).

The current site-directed mutagenesis studies indicate that substitution of mβ3 subunit AA residues in primary face loop C with hβ3 subunit residues enhanced functional expression of mα6mβ2mβ3$^{V9'S}$-nAChRs. In addition, hβ3 subunit AA substitutions in complementary face β2-β3 and E loops for residues in mβ3 subunits increased functional expression of mα6mβ4mβ3-nAChRs. These results are in agreement with the previous observations that substitutions at extracellular N-terminal loops influence functional expression of hα6*-nAChRs and other subtypes of nAChRs (15, 19, 38, 47).

The increased functional expression of mα6*-nAChRs seen upon AA substitution in mβ3 subunits must be due to some combination of increases in efficiency of incorporation of subunits into receptor complexes, trafficking to the cell surface, and/or preservation of cell surface receptors. nAChR mβ3 subunit loop E residues Ser^{144} and Ser^{148} differ from Asn or Val residues, respectively, in hβ3 subunits in side chain length and possibility of engaging in glycosylation (Ser *versus* Asn) and hydrophobicity (Ser *versus* Val) (48). nAChR mβ3 subunit loop C residues Glu^{221} and Phe^{223} differ from Asp or Val AAs in hβ3 subunits in side chain length (Glu *versus* Asp and Phe *versus* Val) and to some degree in hydrophobicity (Phe *versus* Val). These differences in AAs could influence interactions with

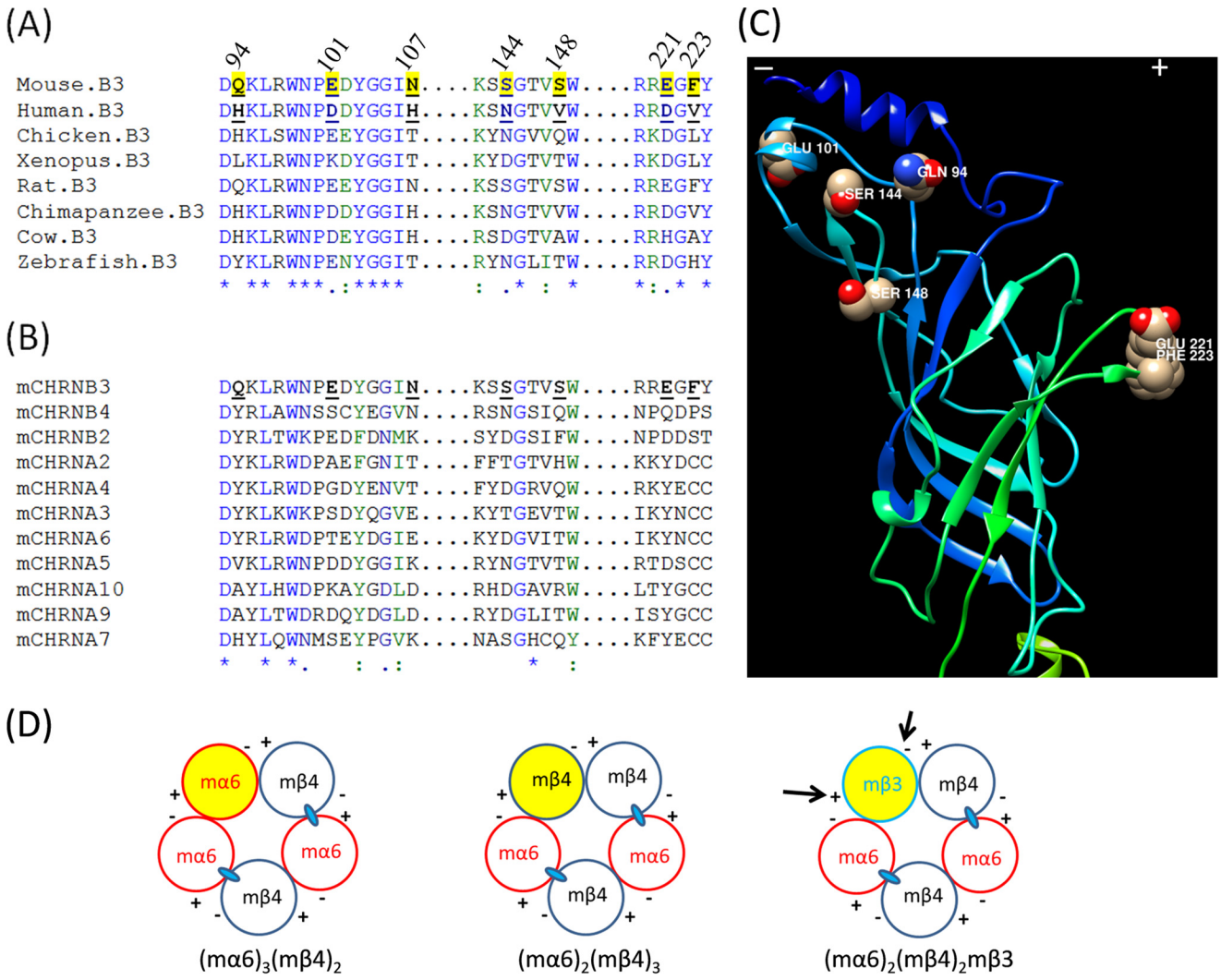

FIGURE 8. **Illustration of nAChR β3 subunit residues and its interfaces that are important in the function of mα6*-nAChRs.** *A*, sequence alignment of nAChR β3 subunit proteins from several species. nAChR β3 protein sequences extracted from GenBank accession numbers NP_ 775304.1 (*Mouse*; *Mus musculus*), NP_000740.1 (*Human*; *Homo sapiens*), NP_990143.1 (*Chicken*; *Gallus gallus*), NP_001080652.1 (*Frog*; *X. laevis*), NP_598281.1 (*Rat*; *Rattus norvegicus*), NP_001029105.1 (*Chimpanzee*; *Pan troglodytes*), XP_599970.2 (*Cow*; *Bos taurus*), and NP_775394.1 (*Zebrafish*; *Danio rerio*) were aligned using ClustalW. *B*, sequence alignment of mouse nAChR β3 subunit proteins. Mouse nAChR subunits were aligned using ClustalW. For both *A* and *B*, numbering begins at the translation start methionine of the mouse nAChR β3 subunit protein and is shown in the N-terminal domain region of interest. *Symbols* below sequences indicate fully (*), strongly (:), or weakly (.) conserved residues, and *underlining* in *shaded* face indicates numbered residues in nAChR mβ3 subunit targeted for mutagenesis studies. *C*, a three-dimensional model of the N-terminal domain of mouse nAChR β3 subunit. A three-dimensional model of the mouse nAChR β3 subunit was generated based on the crystal structure of *Torpedo* muscle nAChR β subunit (Protein Data Bank code 2BG9:B). The N-terminal domain of the nAChR mβ3 subunit possesses β strands that form a β sandwich and conforms to an immunoglobulin fold. AA residues in the β2-β3 loop (Gln^{94} and Glu^{101}), loop E (Ser^{144} and Ser^{148}), or loop C (Glu^{221} and Phe^{223}) that positively influence the current responses of mα6*-nAChRs are identified. The figure displayed was drawn using the program Chimera. *D*, schematic illustration of the composition of mαmβ4*-nAChRs. Adhering to the canonical rule of pentamer formation, mα6mβ4-nAChRs would be formed of three α6 and two β4 subunits (*left*) or two α6 and three β4 subunits (*middle*). In the event mβ3 subunits are integrated into mα6mβ4*-nAChRs, they would substitute for the third mα6 subunit in the first (*left*) configuration or the third mβ4 subunit in the second (*middle*) configuration, occupying what is labeled as the fifth position (*yellow*). Agonist (ACh or nicotine and others) binding sites at the interfaces between α6 and either β2 or β4 subunits are shown as *ovals*. Results from the current study (*right*) support the idea that the β2-β3 loop and loop E residues in the (−) face and/or loop C residues in the (+) face (*arrows*) of the mβ3 subunit are important in higher functional expression of mα6mβ4*-nAChRs. Mouse α6β2*-nAChRs would attain similar configurations, but the β2 subunit would substitute for the β4 subunit.

adjacent (or distant?) β2, β4, or α6 subunits that are important for mα6mβ2*- and mα6mβ4*-nAChR assembly (Fig. 8*D*).

β2-β3 or E loop residues in the negative (−) or complementary face of the mβ3 subunit would be involved in presumed interactions with residues on the positive (+) or primary faces of the neighboring mβ4 or mβ2 subunit, and loop C residues in the positive (+) or primary face of the β3 subunit would be involved in presumed interactions with residues on the negative (−) or complementary faces of the neighboring mα6 subunit in a complex that has the presumed arrangement of $\_(\beta3$ or $\beta3^{V9'S})_+$:$\_\alpha6_+$:$\_(\beta2$ or $\beta4)_+$:$\_\alpha6_+$:$\_(\beta2$ or $\beta4)_+$ where ligand binding pockets are thought to be located between the primary (+) face of mα6 and complementary (−) face of the mβ2 or mβ4 subunits (*i.e.* $\alpha6_+$:$\_\beta4$ or $\alpha6_+$:$\_\beta2$) (Fig. 8). Agonist binding is not expected occur at $\beta3_+$:$\_(\beta2$ or $\beta4)$ or $\beta3_+$:$\_\alpha6$ subunit interfaces. However, recent evidence suggests that interfaces involving subunits in the accessory subunit position where the β3 subunit would be situated can engage in allosteric or co-agonist effects (49–51). Residues in or equivalent to those at mβ3 subunit positions 94, 101, 107, 144, 148, 221, and 223 are

conserved with those in rats but differ from those that are conserved within primates (human and chimp; Fig. 8*A*). These mβ3 subunit AAs also are unique across mouse nAChR subunits (Fig. 8*B*). We have advanced the possibility that these residues could affect efficiency of α6*-nAChR assembly (not altering agonist potency but affecting peak current responses as for mα6*-nAChRs harboring mβ3(S144N/S148V), mβ3(E221D), or mβ3(E221D/F223V) subunits). Another intriguing possibility is that these unique residues could allow formation of novel classes of ligand binding sites at β2/β4:β3 or β3:α6 subunit interfaces that also could lead to changes in levels of receptor function as for ligand occupancy of the α4:α4 subunit interface in low sensitivity α4β2*-nAChR (51).

Plenty of information is available on the role of primary face loops (A, B, and C) from α subunits and complementary face loops (D, E, and F) from β subunits that participate in ligand binding largely from structural and/or mutagenesis studies of muscle-type, α7-, or other nAChRs and from lower eukaryotic and prokaryotic proteins structurally homologous to the extracellular domain of nAChRs (52–54). Our results presented here, for the first time, show that extracellular N-terminal domain loops of the accessory subunit, β3, regulate the functional expression of mα6*-nAChRs. These results also provide further evidence that nAChR β3 subunits not only form functional receptors in combination with nAChR α6 subunits but also can enhance their function by interacting with adjacent subunits mediated by N-terminal loop residues. Current findings lay a foundation for enhanced functional expression of mα6*-nAChRs that could facilitate the discovery and development of nicotinic ligands that selectively interact with α6*-nAChRs. These results could be useful to fuel and inform emerging interest in α6 and β3 subunits and the receptors they compose with specific reference to possible roles in locomotion, reward and reinforcement behavior, schizophrenia, and Parkinson disease (5, 6, 55).

Acknowledgments—We thank Dr. Jerry A. Stitzel (Department of Integrative Physiology, University of Colorado, Boulder, CO) for providing mouse nAChR subunit constructs. We also thank Drs. Doug DeSimone and Todd Stukenberg and Fred Simon of Dr. DeSimone's laboratory (Department of Biology, University of Virginia, Charlottesville, VA) for kind help in establishing and maintaining an X. laevis colony at the University of Virginia Aquatic Animal Center.

REFERENCES

1. Lukas, R. J., Changeux, J. P., Le Novère, N., Albuquerque, E. X., Balfour, D. J., Berg, D. K., Bertrand, D., Chiappinelli, V. A., Clarke, P. B., Collins, A. C., Dani, J. A., Grady, S. R., Kellar, K. J., Lindstrom, J. M., Marks, M. J., Quik, M., Taylor, P. W., and Wonnacott, S. (1999) International Union of Pharmacology. XX. Current status of the nomenclature for nicotinic acetylcholine receptors and their subunits. *Pharmacol. Rev.* **51,** 397–401
2. Wu, J., and Lukas, R. J. (2011) Naturally-expressed nicotinic acetylcholine receptor subtypes. *Biochem. Pharmacol.* **82,** 800–807
3. Hone, A. J., Meyer, E. L., McIntyre, M., and McIntosh, J. M. (2012) Nicotinic acetylcholine receptors in dorsal root ganglion neurons include the α6β4* subtype. *FASEB J.* **26,** 917–926
4. Pérez-Alvarez, A., Hernández-Vivanco, A., McIntosh, J. M., and Albillos, A. (2012) Native α6β4* nicotinic receptors control exocytosis in human chromaffin cells of the adrenal gland. *FASEB J.* **26,** 346–354
5. le Novère, N., Zoli, M., Léna, C., Ferrari, R., Picciotto, M. R., Merlo-Pich, E., and Changeux, J. P. (1999) Involvement of α6 nicotinic receptor subunit in nicotine-elicited locomotion, demonstrated by *in vivo* antisense oligonucleotide infusion. *Neuroreport* **10,** 2497–2501
6. Cui, C., Booker, T. K., Allen, R. S., Grady, S. R., Whiteaker, P., Marks, M. J., Salminen, O., Tritto, T., Butt, C. M., Allen, W. R., Stitzel, J. A., McIntosh, J. M., Boulter, J., Collins, A. C., and Heinemann, S. F. (2003) The β3 nicotinic receptor subunit: a component of α-conotoxin MII-binding nicotinic acetylcholine receptors that modulate dopamine release and related behaviors. *J. Neurosci.* **23,** 11045–11053
7. Drenan, R. M., Grady, S. R., Whiteaker, P., McClure-Begley, T., McKinney, S., Miwa, J. M., Bupp, S., Heintz, N., McIntosh, J. M., Bencherif, M., Marks, M. J., and Lester, H. A. (2008) *In vivo* activation of midbrain dopamine neurons via sensitized, high-affinity α 6 nicotinic acetylcholine receptors. *Neuron* **60,** 123–136
8. Exley, R., Clements, M. A., Hartung, H., McIntosh, J. M., and Cragg, S. J. (2008) α6-containing nicotinic acetylcholine receptors dominate the nicotine control of dopamine neurotransmission in nucleus accumbens. *Neuropsychopharmacology* **33,** 2158–2166
9. Meyer, E. L., Yoshikami, D., and McIntosh, J. M. (2008) The neuronal nicotinic acetylcholine receptors α4* and α6* differentially modulate dopamine release in mouse striatal slices. *J. Neurochem.* **105,** 1761–1769
10. Pons, S., Fattore, L., Cossu, G., Tolu, S., Porcu, E., McIntosh, J. M., Changeux, J. P., Maskos, U., and Fratta, W. (2008) Crucial role of α4 and α6 nicotinic acetylcholine receptor subunits from ventral tegmental area in systemic nicotine self-administration. *J. Neurosci.* **28,** 12318–12327
11. Gotti, C., Guiducci, S., Tedesco, V., Corbioli, S., Zanetti, L., Moretti, M., Zanardi, A., Rimondini, R., Mugnaini, M., Clementi, F., Chiamulera, C., and Zoli, M. (2010) Nicotinic acetylcholine receptors in the mesolimbic pathway: primary role of ventral tegmental area α6β2* receptors in mediating systemic nicotine effects on dopamine release, locomotion, and reinforcement. *J. Neurosci.* **30,** 5311–5325
12. Drenan, R. M., Grady, S. R., Steele, A. D., McKinney, S., Patzlaff, N. E., McIntosh, J. M., Marks, M. J., Miwa, J. M., and Lester, H. A. (2010) Cholinergic modulation of locomotion and striatal dopamine release is mediated by α6α4* nicotinic acetylcholine receptors. *J. Neurosci.* **30,** 9877–9889
13. Xiao, C., Srinivasan, R., Drenan, R. M., Mackey, E. D., McIntosh, J. M., and Lester, H. A. (2011) Characterizing functional α6β2 nicotinic acetylcholine receptors *in vitro*: mutant β2 subunits improve membrane expression, and fluorescent proteins reveal responsive cells. *Biochem. Pharmacol.* **82,** 852–861
14. Kuryatov, A., Olale, F., Cooper, J., Choi, C., and Lindstrom, J. (2000) Human α6 AChR subtypes: subunit composition, assembly, and pharmacological responses. *Neuropharmacology* **39,** 2570–2590
15. Dash, B., Bhakta, M., Chang, Y., and Lukas, R. J. (2011) Identification of N-terminal extracellular domain determinants in nicotinic acetylcholine receptor (nAChR) α6 subunits that influence effects of wild-type or mutant β3 subunits on function of α6β2*- or α6β4*-nAChR. *J. Biol. Chem.* **286,** 37976–37989
16. Cox, B. C., Marritt, A. M., Perry, D. C., and Kellar, K. J. (2008) Transport of multiple nicotinic acetylcholine receptors in the rat optic nerve: high densities of receptors containing α6 and β3 subunits. *J. Neurochem.* **105,** 1924–1938
17. Drenan, R. M., Nashmi, R., Imoukhuede, P., Just, H., McKinney, S., and Lester, H. A. (2008) Subcellular trafficking, pentameric assembly, and subunit stoichiometry of neuronal nicotinic acetylcholine receptors containing fluorescently labeled α6 and β3 subunits. *Mol. Pharmacol.* **73,** 27–41
18. Wang, F., Gerzanich, V., Wells, G. B., Anand, R., Peng, X., Keyser, K., and Lindstrom, J. (1996) Assembly of human neuronal nicotinic receptor α5 subunits with α3, β2, and β4 subunits. *J. Biol. Chem.* **271,** 17656–17665
19. Dash, B., Chang, Y., and Lukas, R. J. (2011) Reporter mutation studies show that nicotinic acetylcholine receptor (nAChR) α5 subunits and/or variants modulate function of α6*-nAChR. *J. Biol. Chem.* **286,** 37905–37918
20. Grinevich, V. P., Letchworth, S. R., Lindenberger, K. A., Menager, J., Mary, V., Sadieva, K. A., Buhlman, L. M., Bohme, G. A., Pradier, L., Benavides, J., Lukas, R. J., and Bencherif, M. (2005) Heterologous expression of human α6β4β3α5 nicotinic acetylcholine receptors: binding properties consis-

tent with their natural expression require quaternary subunit assembly including the α5 subunit. *J. Pharmacol. Exp. Ther.* **312,** 619–626
21. Gerzanich, V., Kuryatov, A., Anand, R., and Lindstrom, J. (1997) "Orphan" α6 nicotinic AChR subunit can form a functional heteromeric acetylcholine receptor. *Mol. Pharmacol.* **51,** 320–327
22. Kuryatov, A., and Lindstrom, J. (2011) Expression of functional human α6β2β3* acetylcholine receptors in *Xenopus laevis* oocytes achieved through subunit chimeras and concatamers. *Mol. Pharmacol.* **79,** 126–140
23. Tumkosit, P., Kuryatov, A., Luo, J., and Lindstrom, J. (2006) β3 subunits promote expression and nicotine-induced up-regulation of human nicotinic α6* nicotinic acetylcholine receptors expressed in transfected cell lines. *Mol. Pharmacol.* **70,** 1358–1368
24. Kuryatov, A., Onksen, J., and Lindstrom, J. (2008) Roles of accessory subunits in α4β2(*) nicotinic receptors. *Mol. Pharmacol.* **74,** 132–143
25. Kuryatov, A., Berrettini, W., and Lindstrom, J. (2011) Acetylcholine receptor (AChR) α5 subunit variant associated with risk for nicotine dependence and lung cancer reduces (α4β2)α5 AChR function. *Mol. Pharmacol.* **79,** 119–125
26. Brown, R. W., Collins, A. C., Lindstrom, J. M., and Whiteaker, P. (2007) Nicotinic α5 subunit deletion locally reduces high-affinity agonist activation without altering nicotinic receptor numbers. *J. Neurochem.* **103,** 204–215
27. Broadbent, S., Groot-Kormelink, P. J., Krashia, P. A., Harkness, P. C., Millar, N. S., Beato, M., and Sivilotti, L. G. (2006) Incorporation of the β3 subunit has a dominant-negative effect on the function of recombinant central-type neuronal nicotinic receptors. *Mol. Pharmacol.* **70,** 1350–1357
28. Jackson, K. J., Marks, M. J., Vann, R. E., Chen, X., Gamage, T. F., Warner, J. A., and Damaj, M. I. (2010) Role of α5 nicotinic acetylcholine receptors in pharmacological and behavioral effects of nicotine in mice. *J. Pharmacol. Exp. Ther.* **334,** 137–146
29. Salas, R., Orr-Urtreger, A., Broide, R. S., Beaudet, A., Paylor, R., and De Biasi, M. (2003) The nicotinic acetylcholine receptor subunit α5 mediates short-term effects of nicotine *in vivo*. *Mol. Pharmacol.* **63,** 1059–1066
30. Dash, B., Bhakta, M., Chang, Y., and Lukas, R. J. (2012) Modulation of recombinant, α2*, α3* or α4*-nicotinic acetylcholine receptor (nAChR) function by nAChR β3 subunits*. *J. Neurochem.* **121,** 349–361
31. Dash, B., and Li, M. D. (2014) Analysis of rare variations reveals roles of amino acid residues in the N-terminal extracellular domain of nicotinic acetylcholine receptor (nAChR) α6 subunit in the functional expression of human α6*-nAChRs. *Mol. Brain* **7,** 35
32. Capelli, A. M., Castelletti, L., Chen, Y. H., Van der Keyl, H., Pucci, L., Oliosi, B., Salvagno, C., Bertani, B., Gotti, C., Powell, A., and Mugnaini, M. (2011) Stable expression and functional characterization of a human nicotinic acetylcholine receptor with α6β2 properties: discovery of selective antagonists. *Br. J. Pharmacol.* **163,** 313–329
33. Dederer, H., Berger, M., Meyer, T., Werr, M., and Ilg, T. (2013) Structure-activity relationships of acetylcholine derivatives with *Lucilia cuprina* nicotinic acetylcholine receptor α1 and α2 subunits in chicken β2 subunit hybrid receptors in comparison with chicken nicotinic acetylcholine receptor α4/β2. *Insect Mol. Biol.* **22,** 183–198
34. Tomizawa, M., Millar, N. S., and Casida, J. E. (2005) Pharmacological profiles of recombinant and native insect nicotinic acetylcholine receptors. *Insect Biochem. Mol. Biol.* **35,** 1347–1355
35. Unwin, N. (2005) Refined structure of the nicotinic acetylcholine receptor at 4Å resolution. *J. Mol. Biol.* **346,** 967–989
36. Guex, N., and Peitsch, M. C. (1997) SWISS-MODEL and the Swiss-PdbViewer: an environment for comparative protein modeling. *Electrophoresis* **18,** 2714–2723
37. Laskowski, R. A., Rullmannn, J. A., MacArthur, M. W., Kaptein, R., and Thornton, J. M. (1996) AQUA and PROCHECK-NMR: programs for checking the quality of protein structures solved by NMR. *J. Biomol. NMR* **8,** 477–486
38. Dash, B., and Lukas, R. J. (2012) Modulation of gain-of-function α6*-nicotinic acetylcholine receptor by β3 subunits. *J. Biol. Chem.* **287,** 14259–14269
39. Groot-Kormelink, P. J., Boorman, J. P., and Sivilotti, L. G. (2001) Formation of functional α3β4α5 human neuronal nicotinic receptors in *Xenopus* oocytes: a reporter mutation approach. *Br. J. Pharmacol.* **134,** 789–796
40. Zwart, R., and Vijverberg, H. P. (1997) Potentiation and inhibition of neuronal nicotinic receptors by atropine: competitive and noncompetitive effects. *Mol. Pharmacol.* **52,** 886–895
41. Parker, J. C., Sarkar, D., Quick, M. W., and Lester, R. A. (2003) Interactions of atropine with heterologously expressed and native α3 subunit-containing nicotinic acetylcholine receptors. *Br. J. Pharmacol.* **138,** 801–810
42. Evans, N. M., Bose, S., Benedetti, G., Zwart, R., Pearson, K. H., McPhie, G. I., Craig, P. J., Benton, J. P., Volsen, S. G., Sher, E., and Broad, L. M. (2003) Expression and functional characterisation of a human chimeric nicotinic receptor with α6β4 properties. *Eur. J. Pharmacol.* **466,** 31–39
43. Champtiaux, N., Han, Z. Y., Bessis, A., Rossi, F. M., Zoli, M., Marubio, L., McIntosh, J. M., and Changeux, J. P. (2002) Distribution and pharmacology of α6-containing nicotinic acetylcholine receptors analyzed with mutant mice. *J. Neurosci.* **22,** 1208–1217
44. Yang, K., Buhlman, L., Khan, G. M., Nichols, R. A., Jin, G., McIntosh, J. M., Whiteaker, P., Lukas, R. J., and Wu, J. (2011) Functional nicotinic acetylcholine receptors containing α6 subunits are on GABAergic neuronal boutons adherent to ventral tegmental area dopamine neurons. *J. Neurosci.* **31,** 2537–2548
45. Exley, R., Maubourguet, N., David, V., Eddine, R., Evrard, A., Pons, S., Marti, F., Threlfell, S., Cazala, P., McIntosh, J. M., Changeux, J. P., Maskos, U., Cragg, S. J., and Faure, P. (2011) Distinct contributions of nicotinic acetylcholine receptor subunit α4 and subunit α6 to the reinforcing effects of nicotine. *Proc. Natl. Acad. Sci. U.S.A.* **108,** 7577–7582
46. Chang, Y., and Weiss, D. S. (1998) Substitutions of the highly conserved M2 leucine create spontaneously opening rho1 γ-aminobutyric acid receptors. *Mol. Pharmacol.* **53,** 511–523
47. Steinbach, J. H. (2011) Flapping loops: roles for hinges in a ligand-binding domain of the nicotinic receptor. *Mol. Pharmacol.* **79,** 337–339
48. Monera, O. D., Sereda, T. J., Zhou, N. E., Kay, C. M., and Hodges, R. S. (1995) Relationship of sidechain hydrophobicity and α-helical propensity on the stability of the single-stranded amphipathic α-helix. *J. Pept. Sci.* **1,** 319–329
49. Moroni, M., Vijayan, R., Carbone, A., Zwart, R., Biggin, P. C., and Bermudez, I. (2008) Non-agonist-binding subunit interfaces confer distinct functional signatures to the alternate stoichiometries of the α4β2 nicotinic receptor: an α4-α4 interface is required for Zn^{2+} potentiation. *J. Neurosci.* **28,** 6884–6894
50. Mazzaferro, S., Benallegue, N., Carbone, A., Gasparri, F., Vijayan, R., Biggin, P. C., Moroni, M., and Bermudez, I. (2011) Additional acetylcholine (ACh) binding site at α4/α4 interface of (α4β2)2α4 nicotinic receptor influences agonist sensitivity. *J. Biol. Chem.* **286,** 31043–31054
51. Eaton, J. B., Lucero, L. M., Stratton, H., Chang, Y., Cooper, J. F., Lindstrom, J. M., Lukas, R. J., and Whiteaker, P. (2014) The unique α4+/−α4 agonist binding site in (α4)3(β2)2 subtype nicotinic acetylcholine receptors permits differential agonist desensitization pharmacology versus the (α4)2(β2)3 subtype. *J. Pharmacol. Exp. Ther.* **348,** 46–58
52. Brejc, K., van Dijk, W. J., Klaassen, R. V., Schuurmans, M., van Der Oost, J., Smit, A. B., and Sixma, T. K. (2001) Crystal structure of an ACh-binding protein reveals the ligand-binding domain of nicotinic receptors. *Nature* **411,** 269–276
53. Miyazawa, A., Fujiyoshi, Y., and Unwin, N. (2003) Structure and gating mechanism of the acetylcholine receptor pore. *Nature* **423,** 949–955
54. Hilf, R. J., and Dutzler, R. (2008) X-ray structure of a prokaryotic pentameric ligand-gated ion channel. *Nature* **452,** 375–379
55. Quik, M., and McIntosh, J. M. (2006) Striatal α6* nicotinic acetylcholine receptors: potential targets for Parkinson's disease therapy. *J. Pharmacol. Exp. Ther.* **316,** 481–489